

# **Changes in brain hierarchy following acute and chronic use of DMT and cannabis**



Robert Tromm | i6272405

Total word count: 12239

Dr. Morten Kringelbach

University of Oxford

Dr. Jan Ramaekers

Maastricht University

A thesis submitted for the degree of

*MSc Cognitive and Clinical Neuroscience, Specialization in Drug  
Development & Neurohealth*

November 2023

To my family for paving a path of abundance for their children.

To my chosen family for their passion, support, and loyalty.

## Acknowledgements

I would be remiss not to begin by expressing my deep gratitude to Oxford for the vast natural beauty and awe-inspiring architecture it has blessed me with in the last few months. My time here has changed me in ways I have not yet begun to process, akin to the grandeur of altered experiences embedded in the pages of this thesis. To Jan, for the trust you placed in me. Overwhelmed, I stepped into your office; with just a few words you introduced me to scientific passions I had no idea were within me. To Morten, for welcoming me with open arms into the Eudaimonia community, and for teaching me scientific rigor, curiosity, criticality, and wisdom. To my family, for the excitement they have for my journey through this academic life. Our lives are so different, and yet you have always shown me unconditional support and understanding. To the wider Eudaimonia community for their generous and gracious support, advice, and friendship. Thank you to Leonardo for solving every silly roadblock I ran into in the darkness of the back office. To Kat, Elvira, Gustavo, Dimitri, Pedro, Fernando, Shamil, Robin, and Joana for the kindness, questions, and critique which allowed me to repair the cracks in my work, and my thinking about the brain and mind. Thank you to the friends I have made since my time in Oxford, whose limitless optimism, curiosity, and love have changed the way I think about friendship, science, and life, and kept me grounded as my mind tripped and fell over the complexities of entropy and hierarchy. Thank you to Michael, Kenneth, Fil, Clayton, Will, Elin, Sebastian, Victoria, and Marilena, whose presence has given me more than can be expressed in words, or at least the limited space I have here. Last but not least, to Maastricht and the psychopharmacology team. To Pablo for holding my hand with patience as I took my first steps in the blinding, expansive world of neuroimaging. A summer I very well could have spent traveling was spent behind my laptop, bashing keys with frustration as FSL threw errors for the thousandth time. I would not change that for anything. Thank you to Petr, who saw the light in me and challenged me to let it out. And to Baptiste, Mila, and Aedan for every moment shared, whether a long night in the library or in Cafe Zondag.

## **Abstract**

Serotonergic psychedelic compounds are gaining an increasing amount of scientific and medical interest for their therapeutic potential and unique effects on consciousness, prompting researchers to consider them as useful tools for probing the neural correlates of consciousness and functional dynamics and organization of the brain. Previous work has revealed that these compounds can significantly alter the functional dynamics and organization of the brain. While substances like cannabis are well-characterized with regard to their chronic effects, a dearth of research has thus far failed to establish alterations in functional dynamics and brain hierarchy following long-term use of psychedelics. A recent proposal has argued that psychedelics act by relaxing high-level priors and flattening the hierarchical organization of the brain. Here, we merge recent work quantifying the hierarchical relationship between the arrow of time and brain dynamics with whole-brain modeling to examine the trophic coherence, a measure of hierarchy, of the brain under ayahuasca, DMT, and cannabis in chronic and occasional users. We recapitulate that psychedelics decrease irreversibility and establish that psychedelics in both long-term users and naive users flatten the brain's hierarchical organization and significantly reconfigure the regional and network-level hierarchical regime, an effect distinct from cannabis in both chronic and occasional users.

# Contents

<b>1</b>	<b>Introduction</b>	<b>1</b>
<b>2</b>	<b>Methods</b>	<b>5</b>
2.1	Data acquisition and preprocessing . . . . .	5
2.1.1	Occasional and chronic users of cannabis . . . . .	5
2.1.2	DMT . . . . .	7
2.1.3	Chronic users of ayahuasca . . . . .	8
2.1.4	Structural connectivity . . . . .	9
2.2	Analysis . . . . .	10
2.2.1	Empirical functional connectivity . . . . .	10
2.2.2	Quantifying causal interactions through the level of irreversibility . . .	10
2.2.3	Generative effective connectivity of the arrow of time . . . . .	12
2.2.4	Trophic coherence . . . . .	13
2.2.5	SVM for condition classification . . . . .	15
2.2.6	Statistical analysis . . . . .	15
<b>3</b>	<b>Results</b>	<b>16</b>
3.1	Irreversibility . . . . .	16
3.2	Trophic coherence of altered states of consciousness . . . . .	18
<b>4</b>	<b>Discussion</b>	<b>26</b>
<b>5</b>	<b>References</b>	<b>34</b>
<b>A</b>	<b>Supplemental Figures</b>	<b>49</b>

## List of Figures

3.1	Trophic coherence provides causal insights into the functional hierarchical organization of the brain on drugs . . . . .	17
3.2	Irreversibility and hierarchy of global brain dynamics under different substances.	18
3.3	Changes in directedness of hierarchical organization under altered states of consciousness . . . . .	20
3.4	Changes in regional hierarchy orchestrating altered states and their common architecture. . . . .	22
3.5	Trophic coherence is an equivalently performing, simpler discriminator of states of consciousness than effective connectivity. . . . .	24
3.6	Directedness of brain functional organization vs. lifetime use and recency of use.	25
A.1	Establishing ideal $\tau$ for each condition. . . . .	50
A.2	Whole-brain model fit. . . . .	51
A.3	Changes in directed connectivity in the psychedelic and cannabis states . . . .	52
A.4	Regional hierarchical levels under baseline and ayahuasca. . . . .	53
A.5	Hierarchical levels under placebo and DMT. . . . .	54
A.6	Hierarchical levels under baseline and cannabis in chronic and occasional users.	55

# Introduction

Psychedelics, including drugs such as psilocybin (4-PO-DMT), lysergic acid diethylamide (LSD), and dimethyltryptamine (DMT), an ingredient in the ritual brew ayahuasca, have seen a massive resurgence in medical and scientific interest in the last decade. These compounds induce significant altered states of consciousness, characterized by vivid imagery, the sense of being in another reality, and dissolution or loosening of the ego, or one's sense of self. Previous research has shown psychedelics to have lasting impacts on personality and mental health outcomes (Barbosa et al., 2009; Griffiths et al., 2008). Personality traits are considered to be rigid and inflexible in healthy adults, and despite this psychedelics have been shown to increase trait openness several months after an acute experience (Griffiths et al., 2011; MacLean et al., 2011; McCrae & Costa Jr., 1997). Evidence is mounting that psychedelics can improve outcomes for a variety of conditions, including depression (Raison et al., 2023), OCD (Moreno et al., 2006), smoking addiction (M. W. Johnson & Griffiths, 2017), and alcohol use disorder (Bogenschutz et al., 2015). The strongest case for the therapeutic efficacy of psychedelics is in the treatment of major depressive disorder (MDD) and treatment-resistant depression (TRD) (R. L. Carhart-Harris et al., 2018; R. Carhart-Harris et al., 2021; Davis et al., 2021; D'Souza et al., 2022; Goodwin et al., 2022; Raison et al., 2023). A similar body of evidence exists for the treatment of psychosocial distress, including depressive and anxiety symptoms, in patients with life-threatening illnesses including cancer (Gasser et al., 2014; Griffiths et al., 2016; Grob et al., 2011; Ross et al., 2016).

The propensity of psychedelics to induce significant altered states also makes them an interesting candidate to assist in understanding normal and abnormal brain function and identifying the neural correlates of consciousness. Previous work has showed that psychedelics modulate emotion (Roseman et al., 2019), sense of self (A. V. Lebedev et al., 2015), perceptual processing (Kometer & Vollenweider, 2016), and increase feelings of connectedness (R. Carhart-Harris et al., 2018). A large body of evidence indicates that psychedelics trigger these effects via 5-HT2a agonism (Nichols, 2016), which are localized in the cortex, primarily in the association cortices (Nichols, 2016; Weber, 2010). It is not well-known what the downstream effects of 5-HT2a agonism are with regard to global brain function, though the rate of research has been growing steadily. Recent work has shown that the therapeutic effects of psychedelics are mediated by TrkB agonism in rodents (Moliner et al., 2023). A convergent body of research has indicated that psychedelics increase measures of brain complexity during the acute psychedelic experi-

ence (A. Lebedev et al., 2016; Tagliazucchi et al., 2014; Viol et al., 2017). These results build support for the theory that, during normal waking consciousness, the human brain operates at sub-criticality, or perfect criticality (R. Carhart-Harris et al., 2014). Criticality has been shown to play a role in a variety of processes in nature, and in the brain it has been speculated to play a role in neuronal avalanches (Beggs & Plenz, 2003). Early studies indicate that psychedelics suppress the default mode network (DMN), decreasing within-network integrity and segregation from other resting-state networks (Buckner et al., 2008; R. L. Carhart-Harris et al., 2012; M. W. Johnson et al., 2019; Müller et al., 2018; Petri et al., 2014; Roseman et al., 2014; Tagliazucchi et al., 2014; Timmermann et al., 2023). Furthermore, decoupling between the DMN and medial temporal lobes has been shown (R. Carhart-Harris et al., 2014), which has led to the suggestion that the effects of psychedelics are mediated by suppression and desegregation of networks in the association cortex (Girn et al., 2022).

The evaluation of long-term outcomes of psychedelic use, as well as the development of an understanding of how psychedelics modulate brain dynamics long-term, has not been extensively demonstrated. Bouso et al. (2015) found significant differences in cortical thickness in midline structures of the brain, with thinning in the middle frontal gyrus, inferior frontal gyrus, precuneus, superior frontal gyrus, superior occipital gyrus, and posterior cingulate cortex (PCC), a key node of the default mode network (DMN). Thickening was found in the precentral gyrus and anterior cingulate cortex. Importantly, the medial prefrontal cortex (mPFC), ACC, and PCC have been associated with the acute effects of psychedelics (Riba et al., 2006), and disruption of the default mode network is a key, convergent finding in psychedelic neuroimaging studies (R. Carhart-Harris & Nutt, 2017; McCulloch et al., 2022). Furthermore, previous work has demonstrated a significant increase in resting-state functional connections across the brain one month after psilocybin use (Barrett et al., 2020). A recent paper by Mallaroni et al. (2023) utilized morphometric similarity network (MSN) analysis, finding that repeated use of ayahuasca was associated with cortical MSN remodelling that was spatially correlated with dysregulation of 5-HT<sub>2a</sub> gene expression.

It's believed that psychedelics shift brain dynamics into a more flexible, diverse, and sensitive mode that is more tuned for information sharing and propagation (Atasoy et al., 2017; R. Carhart-Harris et al., 2014; R. L. Carhart-Harris et al., 2017; Daws et al., 2022; Girn et al., 2022, 2023; Lord et al., 2019; Singleton et al., 2022; Tagliazucchi et al., 2014, 2016; Timmermann et al., 2023) The state of unconstrained cognition induced by psychedelics has been previously conceptualized as a flattening of the attractor landscape – the brain has a reduced tendency to exhibit metastability within potentially maladaptive local minima states, and is thus able to more easily move between metastable local minima (R. Carhart-Harris, 2007; R. Carhart-Harris et al., 2014; Daws et al., 2022; Girn et al., 2023; Kraehenmann, 2017; Kraehenmann et al., 2017; Singleton et al., 2022). This is consistent with the REBUS ('RElaxed Beliefs Under Psychedelics') model of psychedelic action as proposed by R. Carhart-Harris and Friston (2019), which proposes that psychedelics increase entropy in the brain, resulting in 'critical primary states' which

allow for the relaxation of priors and decreased rigidity of thinking and cognition. Entropy is an information-theoretic measure derived from thermodynamics which indexes the fundamental temporal complexity or diversity of a trajectory of the dynamics of a system and the unpredictability of the trajectory, specifically the relative frequency of values that a signal in a system takes on (Girn et al., 2023). It is often characterized more simply as disorder or randomness in a system. Similarly, it is thought that psychedelics flatten the global functional hierarchy of the brain by increasing crosstalk between hierarchical extremes (Girn et al., 2022; Timmermann et al., 2023). Hierarchy here is defined as the directional asymmetry of information flow throughout the brain, or alternatively, the rigidity and stratification of the network (Kringelbach et al., 2023). However, it is difficult to analyze these theories directly, and thus far research has failed to differentiate the action of psychedelics with respect to specific region- or network-wise changes (Girn et al., 2023).

Network theory offers a plethora of approaches to the study of the brain as a complex system, and allows for direct examination of the hierarchical organization of the brain under psychedelics. Previous research has pointed toward the idea that the brain, rather than acting on the world purely through interpretation of environmental stimuli, is constrained by its own dynamics (Buzsáki, 2019). Irreversibility is then a measure of how the external environment drives internal brain dynamics (Buzsáki, 2019; Deco et al., 2022; Kringelbach et al., 2023). By measuring the irreversibility of brain processes, we can estimate the extent to which the environment drives intrinsic dynamics, from there deriving insights about the hierarchical organization of the brain. Previously, Kringelbach et al. (2023) showed improved sensitivity of irreversibility over time-averaged functional connectivity in differentiating between rest and movie-watching conditions with effective connectivity derived from irreversibility over functional connectivity alone, indicating that asymmetry in information flow better captures features of brain dynamics related to distinct states of consciousness. A recent study by Tewarie et al. (2023) showed that irreversibility outperforms functional connectivity in differentiating between brain states with MEG data. A dynamics-based mechanistic explanation of psychedelic action is especially relevant because of the preliminary evidence indicating that changes in dynamics predict psychological and therapeutic outcomes. For example, the degree to which a participant has a mystical experience in a psychedelic session predicts both changes in openness to experience and increases in entropy (A. Lebedev et al., 2016; MacLean et al., 2011).

Here we combine the estimation of entropy production in the brain, irreversibility, with graph theory to examine changes in the functional hierarchical organization of the brain after ayahuasca in a naturalistic study with 24 healthy members of Santo Daime, and DMT in a placebo-controlled study with 17 healthy volunteers with previous psychedelic experience. In contrast to previous work, users of ayahuasca in the original study are extreme with regard to lifetime use of psychedelics (mean = 564, SD = 650). Our main objective was to establish whether psychedelics had an effect on the functional hierarchical organization of the brain, and furthermore whether chronic use of psychedelics alters propensity for changes in hierar-

chical organization and baseline structure. In line with the REBUS and entropic brain models of psychedelic action, we hypothesized that both psychedelics would result in a flattening of the brain's hierarchy under psychedelics (R. Carhart-Harris et al., 2014; R. L. Carhart-Harris, 2019). Furthermore, we contrast these changes with changes in hierarchical organization in chronic and occasional users of cannabis. Previous work in psychedelic research has been limited by the lack of contrast analyses – while novel findings are plentiful and leverage a variety of techniques which converge on similar results, discriminant validity is lacking. We sought to examine how psychedelics might alter the hierarchical organization of the brain differently than cannabis in both chronic and occasional users, especially given the participants under ayahuasca had considerably more lifetime experience than DMT users.

# Methods

## 2.1 Data acquisition and preprocessing

### 2.1.1 Occasional and chronic users of cannabis

**Ethics statement:** This study was conducted according to the code of ethics on human experimentation established by the declaration of Helsinki (1964) and amended in Fortaleza (Brazil, October 2013). The study was approved by the Academic Hospital and University's Medical Ethics Committee (Medical ethical review board Academic Hospital Maastricht/ Maastricht University). All participants gave written informed consent. The Dutch Drug Enforcement Administration gave a permit for the acquisition, storage, and administration of cannabis.

**Participants:** The data acquisition protocols were described in detail in a previous paper (J. Ramaekers et al., 2022). 43 healthy participants with previous experience using cannabis were scanned. For the occasional group, occasional usage was characterized as between one time a month and three times a week. For the chronic group, chronic usage was characterized as at least four times a week. Both were considered only if usage was for the past year. The study was conducted according to a double-blind, placebo-controlled, mixed cross-over design in cannabis users (N=43). Each participant received cannabis placebo and cannabis (300 ug/kg THC) on separate days, separated by a minimum wash-out period of 7 days. Treatment orders were randomly assigned to participants.

Participants received two resting state scans at 15 minutes and 36 minutes after inhalation. The current study was registered in the Netherlands trial register (NTR4894, first date of registration 7/11/2014). Participants in the occasional group were instructed to refrain from drug use, including cannabis (>7 days) and alcohol (>14 hours) prior to the testing day. Participants in the chronic group were given the same instructions, but instructed to refrain from cannabis use only up until 24h before testing day.

**Neuroimaging acquisition for fMRI:** Participants underwent a resting state functional MRI. Images were acquired on a MAGNETOM 7T MR scanner. A total of 258 whole-brain EPI volumes were acquired at rest (TR = 1400ms; TE = 21ms; flip angle = 60 degrees; oblique acquisition orientation; interleaved slice acquisition; 72 slices; slice thickness = 1.5mm; voxel size = 1.5 x 1.5 x 1.5 mm). During scanning, participants were shown a black cross on a white background and were instructed to focus on the cross while attempting to clear the mind.

Results related to the cannabis data included in this manuscript come from analyses performed using CONN (RRID:SCR\_009550) release 22.a and SPM (RRID:SCR\_007037) release 12.7771 (Nieto-Castanon, 2022; Penny et al., 2007; Whitfield-Gabrieli & Nieto-Castanon, 2012).

**Preprocessing:** Preprocessing was performed in line with Luppi et al. (2021). Eight participants were removed due to excessive motion identified by ART as greater than 0.3mm framewise head displacement or global BOLD signal changes above 3 standard deviations. Functional and anatomical data were preprocessed using a flexible preprocessing pipeline including realignment with correction of susceptibility distortion interactions, slice timing correction, outlier detection, direct segmentation and MNI-space normalization, and smoothing (Nieto-Castanon, 2020). Functional data were realigned using SPM realign & unwarp procedure, where all scans were coregistered to a reference image (first scan of the first session) using a least squares approach and a 6 parameter (rigid body) transformation, and resampled using b-spline interpolation to correct for motion and magnetic susceptibility interactions (Andersson et al., 2001; Karl. J. Friston et al., 1995). Temporal misalignment between different slices of the functional data (acquired in interleaved Siemens order) was corrected following SPM slice-timing correction (STC) procedure, using sinc temporal interpolation to resample each slice BOLD timeseries to a common mid-acquisition time (Henson et al., 1999; Sladky et al., 2011). Potential outlier scans were identified using ART as acquisitions with framewise displacement above 0.5 mm or global BOLD signal changes above 3 standard deviations, and a reference BOLD image was computed for each subject by averaging all scans excluding outliers (Nieto-Castanon & Whitfield-Gabrieli, 2022; Power et al., 2014; Whitfield-Gabrieli et al., 2011). Functional and anatomical data were normalized into standard MNI space, segmented into grey matter, white matter, and CSF tissue classes, and resampled to 2 mm isotropic voxels following a direct normalization procedure using SPM unified segmentation and normalization algorithm with the default IXI-549 tissue probability map template (Ashburner, 2007; Ashburner & Friston, 2005; Calhoun et al., 2017; Nieto-Castanon & Whitfield-Gabrieli, 2022). Last, functional data were smoothed using spatial convolution with a Gaussian kernel of 6 mm full width half maximum (FWHM).

**Denoising:** In addition, functional data were denoised using a standard denoising pipeline including the regression of potential confounding effects characterized by white matter timeseries (8 CompCor noise components), CSF timeseries (5 CompCor noise components), motion parameters and their first order derivatives (12 factors), outlier scans (below 163 factors), session and task effects and their first order derivatives (4 factors), and linear trends (2 factors) within each functional run, followed by bandpass frequency filtering of the BOLD timeseries between 0.008 Hz and 0.09 Hz (K. J. Friston et al., 1996; Hallquist et al., 2013; Nieto-Castanon, 2020; Power et al., 2014). CompCor noise components within white matter and CSF were estimated by computing the average BOLD signal as well as the largest principal components orthogonal to the BOLD average, motion parameters, and outlier scans within each subject's eroded segmentation masks (Behzadi et al., 2007; Chai et al., 2012). From the number of noise

terms included in this denoising strategy, the effective degrees of freedom of the BOLD signal after denoising were estimated to range from 78.5 to 296.4 (average 195.6) across all subjects (Nieto-Castanon & Whitfield-Gabrieli, 2022).

### 2.1.2 DMT

**Ethics:** All participants provided written informed consent for participation in the study. The study was approved by the National Research Ethics Committee London-Brent and the Health Research Authority, and was conducted under the guidelines of the revised Declaration of Helsinki (2000), the International Committee on Harmonization Good Clinical Practices guidelines, and the National Health Service Research Governance Framework. Imperial College London sponsored the research, which was conducted under a Home Office license for research with Schedule I drugs.

**Participants:** The data acquisition methods were described in a previous paper, but will be briefly reported here (Timmermann et al., 2023). The study was a single-blind, placebo-controlled, counter-balanced design. Volunteers participated in two testing days, separated by two weeks. Participants were tested for drugs of abuse and involved in two separate scanning sessions on each test day. In the initial, task-free session, participants received intravenous (IV) administration of either placebo (10mL sterile saline) or 20mg DMT fumarate (in 10mL sterile saline) injected over 30 seconds. Resting-state sessions lasted 28 minutes with DMT or placebo administered at the end of the 8th minute and scanning was over 20 minutes after injection. Participants laid in the scanner with an eye mask on. A second session was followed with the same procedure as the first.

**Neuroimaging Acquisition for fMRI:** Images were acquired with a 3T Siemens Magnetom Verio syngo MR B17 scanner using 12-channel head coil for compatibility with EEG acquisition. Functional imaging was carried out with a T2\*-weighted BOLD-sensitive gradient echo planar imaging sequence (TR = 2000 ms, TE = 30ms, TA = 28.06 ms, flip angle = 80 degrees, voxel size = 3 x 3 x 3mm, 35 slices, interslice distance = 0mm). Whole brain T1-weighted structural images were also acquired.

**Preprocessing:** Preprocessing was performed with the same steps as occasional and chronic users of cannabis. Four participants were removed due to excessive motion identified by ART as greater than 0.3mm framewise head displacement or global BOLD signal changes above 3 standard deviations. Denoising was performed with the same standard denoising pipeline, including regression of potential confounding effects characterized by white matter time-series (5 CompCor noise components), CSF time-series (5 CompCor noise components), motion parameters and their first and second order derivatives (18 factors), outlier scans (below 236 factors), session and task effects and their first order derivatives (4 factors), and linear trends (2 factors) within each functional run, followed by bandpass frequency filtering of the BOLD timeseries between 0.008 Hz and 0.09 Hz (K. J. Friston et al., 1996; Hallquist et al., 2013; Nieto-Castanon,

2020; Power et al., 2014). CompCor noise components within white matter and CSF were estimated by computing the average BOLD signal as well as the largest principal components orthogonal to the BOLD average, motion parameters, and outlier scans within each subject's eroded segmentation masks (Behzadi et al., 2007; Chai et al., 2012). From the number of noise terms included in this denoising strategy, the effective degrees of freedom of the BOLD signal after denoising were estimated to range from 413 to 520.5 (average 489.6) across all subjects (Nieto-Castanon & Whitfield-Gabrieli, 2022).

### 2.1.3 Chronic users of ayahuasca

**Ethics statement:** The study was conducted according to the code of ethics on human experimentation established by the Declaration of Helsinki (1964) and amended in Fortaleza (Brazil, October 2013) and in accordance with the Medical Research involving Human Subjects Act (WMO) and was approved by the Academic Hospital and University's Medical Ethics committee (Medical ethical review board Academic Hospital Maastricht/Maastricht University) (NL70901.068.19/METC19.050). All participants were fully informed of all procedures, possible adverse reactions, legal rights and responsibilities, expected benefits, and their right to voluntary termination without consequences.

**Participants:** The data acquisition protocols were described in detail in a previous paper (Mallaroni et al., 2022). Twenty four participants were enrolled in a within-subject, fixed-order observational study. The cohort consisted of experienced members of the Dutch chapter of the church Santo Daime. Participants underwent two consecutive test days – one baseline followed by another under the influence of ayahuasca. Participants administered to themselves a volume of ayahuasca equivalent to their usual dose (0.045 mg/kg), prepared from a single batch by the Church of Santo Daime and analyzed according to referencing standards (see previous paper for details). To facilitate and naturalize the study, participants drank ayahuasca while initiating the works in company of fellow members. Dosing schedules were stratified across lab visits with testing performed within 4 pairs of visits, with 6 subjects per cycle. The brew used contained 0.14 mg/mL DMT, 4.50mg/ML harmine, 0.51mg/mL harmaline, and 2.10 mg/mL tetrahydro-harmine. Ceremonies were organised and supervised by the Santo Daime church. The research term at Maastricht University was not involved in the organization of the rituals, production, dosing, or administration of ayahuasca.

**Neuroimaging acquisition for fMRI:** Participants underwent resting state functional MRI. Images were acquired on a MAGNETOM 7T MR scanner. Participants underwent a structural MRI (60 minutes post-treatment), single-voxel proton MRS in the PCC (70 minutes post-treatment), visual cortex (80 minutes post-treatment), and fMRI (90 minutes post-treatment) during peak subjective effects. T1-weighted anatomical images were acquired with magnetization-prepared 2 rapid acquisition gradient-echo (MP2RAGE) sequence (TR = 4500ms, TE = 2.39 ms, TI1 = 900ms, TI2 = 2750ms, flip angle 1 = 5 degrees, flip angle 2 = 3 degrees, voxel size =

0.9 mm isotropic, matrix size = 256 x 256 x 192, phase partial Fourier = 6/8, GRAPPA = 3 with 24 reference lines, bandwidth = 250 Hz/pixel). 500 whole brain echo planar (EPI) volumes were acquired at rest (TR = 1400ms; TE = 21ms; field of view = 198mm; flip angle = 60 degrees; oblique acquisition orientation; interleaved slice acquisition; 72 slices; slice thickness = 1.5mm; voxel size = 1.5 x 1.5 x 1.5 mm) followed by 5 phase encoding volumes for EPI unwarping. Participants were shown a black cross on a white background and were instructed to focus on the cross during EPI acquisition.

Results related to the ayahuasca data included in this manuscript come from analyses performed using CONN (RRID:SCR\_009550) release 21.a and SPM (RRID:SCR\_007037) release 12.7771 (Nieto-Castanon, 2022; Penny et al., 2007; Whitfield-Gabrieli & Nieto-Castanon, 2012).

**Preprocessing:** Preprocessing was performed with the same steps as occasional and chronic users of cannabis. No participants were removed due to excessive motion identified by ART as greater than 0.3mm framewise head displacement or global BOLD signal changes above 3 standard deviations. Denoising was performed with the same standard denoising pipeline, including regression of potential confounding effects characterized by white matter time-series (5 CompCor noise components), CSF time-series (5 CompCor noise components), motion parameters and their first and second order derivatives (18 factors), outlier scans (below 206 factors), session and task effects and their first order derivatives (4 factors), and linear trends (2 factors) within each functional run, followed by bandpass frequency filtering of the BOLD timeseries between 0.008 Hz and 0.09 Hz (K. J. Friston et al., 1996; Hallquist et al., 2013; Nieto-Castanon, 2020; Power et al., 2014). CompCor noise components within white matter and CSF were estimated by computing the average BOLD signal as well as the largest principal components orthogonal to the BOLD average, motion parameters, and outlier scans within each subject's eroded segmentation masks (Behzadi et al., 2007; Chai et al., 2012). From the number of noise terms included in this denoising strategy, the effective degrees of freedom of the BOLD signal after denoising were estimated to range from 139.1 to 214 (average 202.2) across all subjects (Nieto-Castanon & Whitfield-Gabrieli, 2022).

#### 2.1.4 Structural connectivity

To reconstruct a structural connectivity matrix for whole-brain modelling, we obtained multi-shell diffusion-weighted imaging data from 32 participants from the HCP database (scanned approx. 89 minutes) (Kringelbach et al., 2023). Acquisition parameters are described in detail on the HCP website (Setsompop et al., 2013). Diffusion tensor imaging data was parcellated according to the aforementioned DBS80 scheme. The connectivity matrix was weighted.

## 2.2 Analysis

Trophic coherence is a graph-theoretic approach which allows us to infer the directedness and hierarchical levels for each brain region across the brain through the conversion of effective weighting of the existing anatomical connectivity, as derived by a causal mechanistic whole-brain model, into a directed graph (S. Johnson et al., 2014; MacKay et al., 2020). This allows for examination of changes in the functional hierarchical organization of the brain across varying conditions.

### 2.2.1 Empirical functional connectivity

The functional connectivity (FC)  $FC_{ij}^{empirical}$  is a matrix of Pearson correlations across the fMRI BOLD timeseries activity between brain regions,  $i$  and  $j$ , in different conditions. Spatially normalized brains (MNI-space) were parcellated into 62 cortical regions from the Mindboggle-modified Desikan-Killiany parcellation (Desikan et al., 2006; Klein & Tourville, 2012), with the addition of 18 subcortical regions (9 regions per hemisphere) including the hippocampus, amygdala, subthalamic nucleus (STN), globus pallidus internal segment (GPi), global pallidus external segment (GPe), putamen, caudate, nucleus accumbens, and thalamus from the Gasser parcellation (Glasser et al., 2016). This parcellation is referred to synonymously in previous literature as the DBS80 or DK80 parcellation (Capouskova et al., 2022; Deco, Vidaurre, & Kringelbach, 2021; Desikan et al., 2006; Gomes et al., 2020; Klein & Tourville, 2012; Kringelbach et al., 2023).

### 2.2.2 Quantifying causal interactions through the level of irreversibility

Previous research has shown that capturing the asymmetry in a temporal process, the arrow of time, by comparing time-shifted correlations between the forward and reversed BOLD fMRI time-series provides a quantification of the level of irreversibility & the degree of non-equilibrium in brain dynamics, as well as the degree to which one brain region is driving another (Deco et al., 2022; Kringelbach et al., 2023). An increase in irreversibility is associated with increased directionality of information flow and a resulting high level of hierarchical reorganization. It is by this notion that asymmetry in the directionality of information flow allows for determination of asymmetry in both space and time, resulting in distinct spatiotemporal hierarchies (Deco, Cruzat, & Kringelbach, 2019; Golesorkhi et al., 2021; Kobeleva et al., 2021).

By definition, non-hierarchical processes are in detailed balance and are fully reversible processes. In contrast, hierarchical processes have irreversible trajectories and result in the production of entropy. Production entropy is quantified as the Kullback-Leibler distance between the forward and backward transition probability of the dynamic evolution of a system. We leveraged the asymmetry of information flow, calculating the time-shifted correlation between each voxel across the brain for both the forward and reversed time-series. The asymmetry be-

tween time-series reflects the time-dependency of causal interactions between regions of interest, and irreversibility can be evaluated as the absolute quadratic difference between the pairwise time-shifted correlation between forward and reversed time-series. Through this, irreversibility queries the production entropy of the brain (Lynn et al., 2021; Sanz Perl et al., 2021).

The construction of the reversed time-series is done simply by reversing the natural forward evolution of the BOLD signal for each voxel across the space of the brain. The causal dependency between two time-series  $x(t)$  and  $y(t)$  is measured through the time-shifted correlation

$$c_{forward}(\Delta t) = \langle x(t), y(t + \Delta t) \rangle \quad (2.1)$$

and for the reversed time-series the time-shifted correlation is given by (Deco et al., 2022; Kringelbach et al., 2023):

$$c_{reversed}(\Delta t) = \langle x^r(t), y^r(t + \Delta t) \rangle \quad (2.2)$$

At a given time  $\Delta t = T$ , the level of irreversibility can be computed as the absolute difference between the correlations of the forward and reversed time-series, respectively.  $\Delta t$  represents the time shifting parameter  $T$ :

$$I_{x,y}(T) = |c_{forward}(T) - c_{reversal}(T)| \quad (2.3)$$

The value of  $T$  is given by iterating through values of  $T$  and identifying the value which provides the strongest difference between conditions for each dataset. Maximal differences between the correlation of the forward and reversed time-series can be found when one time-series has a strong dependency on time that the other does not. The forward  $x_i(t)$  and reversal  $x_i^{(r)}(t)$  matrices are defined in the multidimensional case as the dynamical evolution of the variable describing the system, wherein  $i$  represents the different dimensions of the system. The functional causal dependencies for the forward and reversed matrices are then expressed by the normalized mutual information based on their respective time-shifted correlations:

$$FS_{forward,ij}(\Delta t) = -\frac{1}{2} \log[1 - \langle x_i(t), x_j(t + \Delta t) \rangle^2] \quad (2.4)$$

$$FS_{reversal,ij}(\Delta t) = -\frac{1}{2} \log[1 - \langle x_i^{(r)}(t), x_j^{(r)}(t + \Delta t) \rangle^2] \quad (2.5)$$

where FS is the functional similarity between  $x_i(t)$  and  $x_j(t + \Delta t)$ . Mutual information is utilized as the relationship between variables in the multi-dimensional time-series is not necessarily linear. The absolute quadratic difference of these matrices is the irreversibility matrix

$$I = \|FS_{forward}(T) - FS_{reversal}(T)\|_2 \quad (2.6)$$

where  $I$  is the mean value of the absolute squares of the difference between the forward and

reversed matrices. If the difference matrix is defined as such

$$FS_{diff,ij} = [FS_{forward,ij}(T) - FS_{reversal,ij}(T)]^2 \quad (2.7)$$

then the matrix is simply the square of the elements of the difference between the forward and reversal matrices. The level of NR,  $I$ , is then the mean of the elements of  $FS_{diff}$ . A simple measure of hierarchy is the standard deviation of  $I$ , which measures the variability in the asymmetry of brain activity.

### 2.2.3 Generative effective connectivity of the arrow of time

As previously described by Kringelbach et al. (2023), local dynamics of each brain region are described by the normal form of a supercritical Hopf bifurcation. The whole-brain dynamics are given by coupling nodes through the inclusion of a diffusive coupling term, common difference coupling, representing the input received by a region  $n$  from every other region  $p$ , weighted by the GEC,  $G_{np}$ . The dynamics of individual nodes are given by the normal form of a supercritical Hopf bifurcation in Cartesian coordinates with an additive Gaussian noise  $\eta_n(t)$  and standard deviation  $\beta$ :

$$\frac{dx_n}{dt} = [a_n - x_n^2 - y_n^2]x_n - \omega_n y_n + \sum_{p=1}^N G_{np}(x_p - x_n) + \beta\eta_n(t) \quad (2.8)$$

$$\frac{dy_n}{dt} = [a_n - x_n^2 - y_n^2]y_n + \omega_n x_n + \sum_{p=1}^N G_{np}(y_p - y_n) + \beta\eta_j(t) \quad (2.9)$$

The normal form has a supercritical bifurcation  $a_n = 0$ , where when  $a_n > 0$ , the system is engaged in a stable limit cycle with frequency  $f_n = \omega_n/2\pi$ . When  $a_n < 0$ , local dynamics are in a stable fixed point which represents the low activity noise state. Intrinsic frequencies  $\omega_n$  are estimated from the data given by the averaged peak frequency of narrowband BOLD signals of each brain region ( $n = 1, \dots, 80$ ). The best fit for  $a_n$  will be calculated after model estimation. The noise factor  $\beta$  is set, by default, to 0.01.

The whole-brain model was constructed by fitting the existing anatomical connectivity to the empirical functional connectivity (FC) matrix and the time-delayed covariance matrix, or the covariance of irreversibility. Effective connectivity was simulated for the ayahuasca users, DMT users, and occasional and chronic cannabis users. Optimization of the GEC between brain regions is performed by comparing the output of the model with empirical measures of the forward and reversed time-shifted correlations and the whole-brain functional connectivity. A heuristic gradient descent algorithm is used to update and optimize the fit of the GEC, error estimated by mean squared error between the empirical and simulated functional connectivity matrix and covariance of irreversibility. All values are transformed into mutual information, assuming Gaussianity, to work only positive values:

$$G_{ij} = G_{ij} + \epsilon(FS_{ij}^{empirical} - FS_{ij}^{model}) - \epsilon' \left\{ \left[ FS_{forward,ij}(T) - FS_{reversal,ij}(T) \right] - \left[ FS_{forward,ij}^{model}(T) - FS_{reversal,ij}^{model}(T) \right] \right\} \quad (2.10)$$

$FS_{ij}$  is based on the functional connectivity matrix  $FC_{ij}$  as mutual information obtained by:

$$FS_{ij} = -\frac{1}{2} \log[1 - (FC_{ij})^2] \quad (2.11)$$

The model was initialized with the anatomical connectivity obtained from probabilistic tractography from dMRI and iterated with the updated GEC until the fit converged toward a stable value  $a_n$ , with  $\epsilon = 0.0005$  and  $\epsilon' = 0.0001$ . Only known existing connections in either hemisphere were updated, with one exception – the algorithm also updates homolog connections between the same regions in either hemisphere, given that tractography is less accurate when accounting for this connectivity. Model results are computed for each participant, and averaged over as many simulations as there are participants for each condition. The model was linearized with the addition of a Jacobian matrix for steady state estimation. Updated covariance matrices and functional connectivity matrices were calculated by solving the Sylvester equation for the Jacobian with noise covariances.

## 2.2.4 Trophic coherence

The GEC matrix represents the effective weighting between different nodes. In other words, it provides connection strengths as edges between brain regions. The advantage of utilizing a whole-brain model to construct the effective connectivity of the FC and the NR matrix is that it allows for causal inference of the directionality of influence that one region in the brain has on another. Trophic coherence is a property of directed graphs that has been previously used as a statistical predictor of the linear stability of food webs, but can be applied to any directed graph (S. Johnson et al., 2014; MacKay et al., 2020). Here we use an improved notation of trophic coherence, first introduced by MacKay et al. (2020), that allows for non-existence of basal nodes (a node with no incoming edges) and the examination of reverse flows – this is important for brain networks, as brain regions do not simply interact in a feed-forward manner, but have feedback loops and self-loops.

If we consider a directed network with a set  $N$  of nodes and set  $E$  of edges, we can suppose there is at most one edge from node  $m$  to node  $n$ , with the possibility of an edge from  $n$  to  $m$  as well. Each edge has some weight  $w_{mn} > 0$ . This describes the effective weighting, or functional influence, of one brain region on another. If an edge does not exist between a node  $m$  and  $n$ , we denote this with  $w_{mn} = 0$ . We then define the in-degree and out-degree for each node  $n$  as

$$w_n^{in} = \sum_m w_{nm} \quad \text{and} \quad w_n^{out} = \sum_m w_{mn}. \quad (2.12)$$

The total weight of each node  $n$  is denoted as

$$u_n = w_n^{in} + w_n^{out}, \quad (2.13)$$

which can be given alternatively by the sum of sum of rows and columns, respectively, for a weighted matrix  $W$ , where the sum of rows represents the vectorized in-degree, and sum of columns represents the vectorized out-degree. The imbalance for each node  $n$  is given by

$$v_n = w_n^{in} - w_n^{out}, \quad (2.14)$$

which can be alternatively provided by the difference between sum of rows and sum of columns for  $W$ . The weighted graph-Laplacian operator  $\Lambda$  can be defined in matrix form by

$$\Lambda = \text{diag}(u) - W - W^T, \quad (2.15)$$

where  $T$  is the transpose of the weighted matrix  $W$ . The hierarchical levels for each brain region can then be solved from the solution  $\gamma$  for the linear system of equations

$$\Lambda\gamma = v. \quad (2.16)$$

To force the system to always have a unique solution, it is possible to add an arbitrary constant to one edge of the network. Specifically, one must add an arbitrary constant to each connected component of the network, or the maximal subset of the network where one can move, ignoring direction of edges, between any node  $m$  and  $n$  in the component. Though anatomical connectivity is sparse in the brain, there is only one connected component by definition. In our case, we used the self-loop in the first node. Furthermore, one can normalize the hierarchical levels, thereby also creating a basal node in the network, by subtracting from each hierarchical level the minimum of the vector  $\gamma$ . Following this, trophic incoherence can be given by

$$F_0 = 1 - \frac{\sum_{mn} w_{mn}(\gamma_n - \gamma_m - 1)^2}{\sum_{mn} w_{mn}}. \quad (2.17)$$

The trophic coherence is then defined by  $1 - F_0$ . A network is considered to be maximally coherent if  $F_0 = 0$  and maximally incoherent if  $F_0 = 1$ . Maximally coherent networks have nodes that fall evenly onto defined trophic levels, while incoherent networks have many nodes lying on fractional trophic levels. We can then treat trophic coherence as the directedness of the network.

Emphasis was placed on robust connections and achieved by thresholding weighting between regions such that only edges with  $w_{mn} > 0.015$  are considered to have an existing con-

nection for visualization purposes. Statistical analysis is carried out with weak edges intact as weak connections often represent important connections between clusters.

### 2.2.5 SVM for condition classification

We used a error-correcting output code support vector machine as implemented with the MATLAB function `fitcecoc`, with 90% training and 10% validation split. We optimized hyperparameters with automatic settings and utilized `expected-improvement-plus` as an acquisition function. The function returns a fully trained model utilizing the predictors in the input with class labels. We then cross-validated the model with 20 k-fold cross-validation, and evaluated the general error and accuracy. The SVM uses inputs for each dataset and for all datasets and conditions, to predict differences in the distribution of hierarchical levels across baseline and acute administration conditions, as well as between occasional and chronic users of ayahuasca/DMT and cannabis.

### 2.2.6 Statistical analysis

Changes in irreversibility, hierarchy, and trophic coherence were calculated for each condition with a Wilcoxon signed-rank test with  $\alpha = 0.05$  as the threshold for statistical significance, implemented in the R package `ggsignif` (Constantin & Patil, 2021; R Core Team, 2023; Wickham et al., 2019). For ayahuasca, a linear mixed-effects model was fit to irreversibility, hierarchical levels, and trophic coherence in order to control for varying dosages between subjects. Effect sizes reported as Cohen's d with 95% confidence intervals.

We then fit a linear mixed-effects model to the ayahuasca data with ayahuasca or baseline condition as the outcome variable with time since last ceremony (recency) and the number of total ceremonies, as well as their interaction, as fixed effects, and max DMT concentration in the blood (ng/ml) as a covariate. Individual subject variance at the intercept was allowed in the model. Linear fit was determined with the MATLAB function `polyfit` and  $R^2$  as the squared correlation coefficient.

Changes across conditions for the full 80 regions and 7 resting-state network hierarchical levels were obtained via a three-step process. Non-parametric, two-tailed 10,000 iteration permutation testing was performed for each region or functional network with a p-threshold of 0.01. For the resting-state network analysis, 5,000 permutations were used. Benjamini-Hochberg False Discovery Rate was used with a threshold of 0.2 to identify false discoveries and correct for multiple comparisons (Benjamini & Hochberg, 1995) for the full number of parcels, and 0.05 for resting-state networks.

# Results

Examining the changes in orchestration of brain function through hierarchy induced by ayahuasca and DMT allows for a deeper look into the mechanisms of psychedelic action, adding nuance to existing theories and bridging the gap between the profound alterations in consciousness resulting from psychedelics and their biological effects. Furthermore, we aimed to add further evidence to a recent unified model of psychedelic action on the brain (R. Carhart-Harris & Friston, 2019). Figure 3.1 describes the overall framework employed in this study. Participants were scanned and BOLD timeseries for each region of a coarse-grained parcellation, the Mindboggle-modified Desikan-Killiany with subcortical regions (DK80), were extracted. Production entropy is estimated via irreversibility by exploiting the fact that hierarchical processes necessarily produce entropy. Irreversibility in timeseries is extracted from the asymmetry between forward and reversed timeseries through the addition of a time delay in correlations between regions. The irreversibility is then used to fit a whole-brain Hopf model, the generative effective connectivity (GEC). Finally, we decompose the resultant effective connectivity graph into the directedness and regional brain hierarchy by trophic coherence.

## 3.1 Irreversibility

To determine the effects of ayahuasca, DMT, and cannabis on BOLD fMRI-derived brain hierarchy, we first computed irreversibility, an estimate of production entropy. Irreversibility provides a quantification of how the environment is differentially driving brain dynamics out of equilibrium depending on the underlying brain state (Deco et al., 2022; Kringelbach et al., 2023). This is especially relevant within the context of the psychedelic experience and associated changes in brain dynamics from long-term use as psychedelics are known to modulate sensitivity to the environment and extrinsic stimuli, which is consistent with the role of serotonergic neurotransmission in environmental sensitivity regulation (Branchi, 2011; R. L. Carhart-Harris et al., 2017).

We analyzed irreversibility over an 8-minute period after the injection of DMT or placebo, ~12-minute period 1h after the oral ingestion of ayahuasca, and 6-minute period beginning 15 minutes after inhalation of cannabis or placebo. The ideal time delay was calculated by finding the value that most effectively discriminated between conditions (see Figure A.1). Compared with baseline and placebo conditions, irreversibility was found to be reduced significantly for

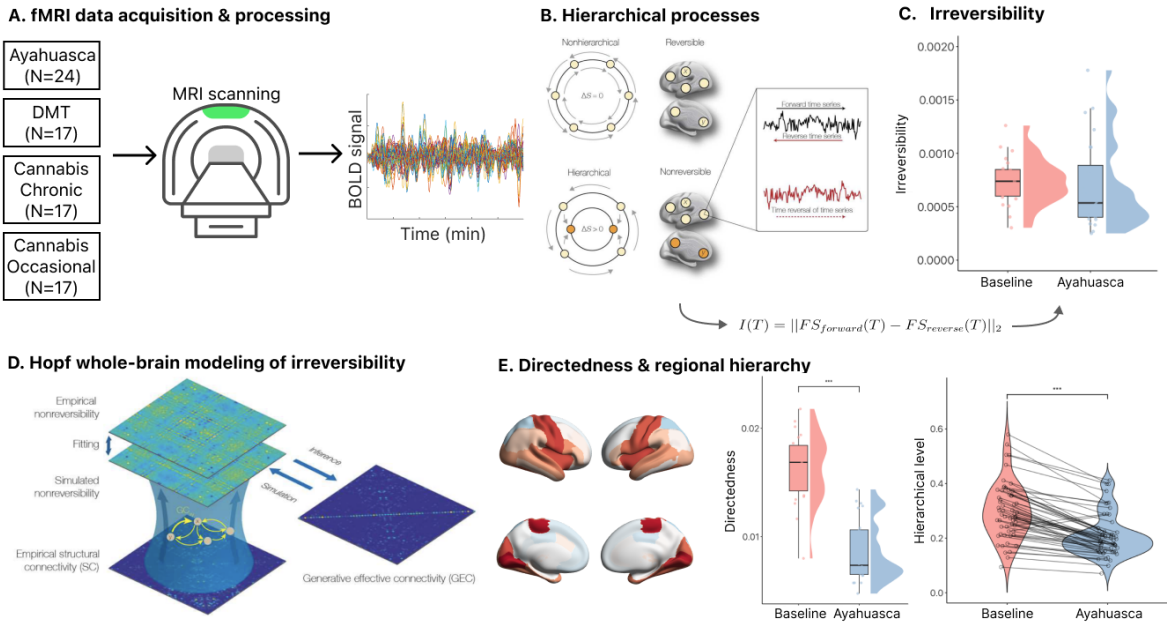


Figure 3.1: Trophic coherence provides causal insights into the functional hierarchical organization of the brain on psychedelics and cannabis. The figure shows the overall methodological flow presented in this present study. (A). Participants in three datasets (ayahuasca, DMT, chronic and occasional use of cannabis) were scanned during peak experiences with fMRI (see Methods for acquisition details). BOLD timeseries were extracted after preprocessing. (B). Hierarchical processes produce entropy via irreversible flow of information. Non-hierarchical systems are in detailed balance and fully reversible, whereas hierarchical systems break detailed balance. Irreversibility in time-series can be extracted from the asymmetry between forward and reversed timeseries, shifted in time. (C) Irreversibility is computed as mutual information, represented by the absolute quadratic difference, between the time-shifted pairwise correlation of the forward and reversed timeseries, across all voxels in the brain. Irreversibility is given by the IR matrix, and hierarchy is represented as the variability of asymmetry in underlying causal interactions for each participant in each condition (see Methods). (D). The irreversibility and structural anatomical connectivity derived from diffusion tensor imaging (DTI) are used to fit a whole-brain Hopf model, estimating the effective connectivity of irreversibility (see Methods). (E). The hierarchical influence of each region in the brain over others (left, right) and the overall trophic coherence, or directedness, of hierarchical organization (middle), are given through trophic coherence (see Methods). Wilcoxon signed-rank test, middle panel. Non-parametric two-sample permutation-based test followed by False Discovery Rate, right panel. (\* p<0.05; \*\* p<0.01; \*\*\* p<0.001)

DMT ( $Z=2.79$ ,  $d = 1.05$  [0.32 1.77],  $p = 0.0052$ ) and chronic use of cannabis ( $Z=2.79$ ,  $d= 1.05$  [0.32 1.77],  $p = 0.0052$ ) across the whole brain (Figure 3.2a). Non-significant trends toward decrease were found for ayahuasca ( $p = 0.41$ ) and occasional use of cannabis ( $p = 0.14$ ). A measurement of hierarchy was derived from the standard deviation of irreversibility for each subject (Figure 3.2b). These results suggest that DMT and chronic use of cannabis decrease the weight of extrinsic dynamics, or the environment, on intrinsic brain dynamics.

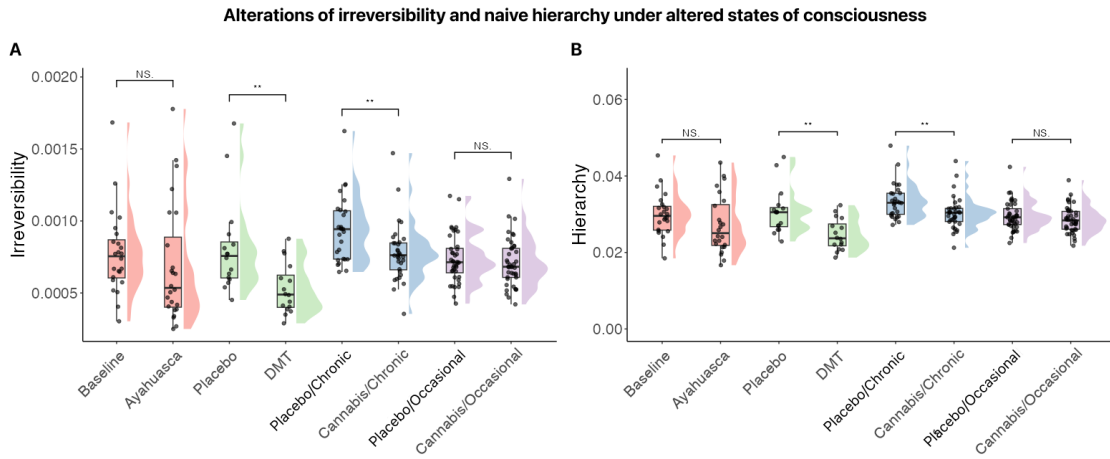


Figure 3.2: Irreversibility and hierarchy of global brain dynamics under different substances. (A) Global irreversibility across 80 regions of the DBS80 for ayahuasca, DMT, chronic use of cannabis, and occasional use of cannabis. Significant decreases, as evaluated by non-parametric Wilcoxon signed-rank test, were found for DMT>Placebo ( $Z=2.79$ ,  $d = 1.05$  [0.32 1.77],  $p = 0.0052$ ) and the chronic use of cannabis ( $Z=2.79$ ,  $d= 1.05$  [0.32 1.77],  $p = 0.0052$ ), but not occasional use ( $p = 0.14$ ). A nonsignificant trends toward decrease in irreversibility was found for ayahuasca ( $p = 0.41$ ) (B) Similar results were found for a simple measure of hierarchy, defined as the standard deviation of irreversibility. Significant differences were found for the change in irreversibility from placebo to DMT ( $Z = 2.74$ ,  $d = 1.14$  [0.40 1.86],  $p = 0.0061$ ), and from baseline to acute cannabis experience for chronic users ( $Z = 2.32$ ,  $d = 0.69$  [0.17 1.20],  $p = 0.02$ ). Nonsignificant decreases in hierarchy were found for ayahuasca ( $p = 0.15$ ) and occasional users of cannabis ( $p = 0.21$ ). (\*  $p<0.05$ ; \*\*  $p<0.01$ ; \*\*\*  $p<0.001$ ).

### 3.2 Trophic coherence of altered states of consciousness

This first-pass analysis showed that changes in irreversibility, an indirect measure of hierarchy, are present under both psychedelic and cannabis conditions. We further examined changes in hierarchy by analyzing the effective connectivity through whole-brain modelling with generative effective connectivity (GEC) (Kringelbach et al., 2023). Irreversibility provides information about whether or not hierarchical, or directional, information flow exists between two regions, but does not inform one of which direction that information is moving in. The framework presented here, first implemented by Deco et al. (2022), is less computationally expensive than alternatives including direct estimation of the entropy rate through methods like transfer entropy for measuring Granger causality, and deep learning models (Deco, Perl, et al., 2021; Lynn et al., 2021; Sanz Perl et al., 2021; Seif et al., 2021). Furthermore, this framework has been shown to estimate precise signatures of different brain states in both electrocorticography (ECoG) data from non-human primates, including awake, deep sleep, and anesthesia, as well as differentiating between tasks, rest, and movie-watching in humans (Deco et al., 2022; Kringelbach et al., 2023).

The model-free quantification of the level of irreversibility is used as a basis by which to fit

a causal, mechanistic whole-brain model, which provides the effective weighting of the existing structural connectivity as derived from diffusion tensor imaging (K. J. Friston et al., 2003). Here, we derived anatomical connectivity from the Human Connectome Project with 32 participants. This presents a limitation, as anatomical connectivity is known to vary across individuals and may result in a less accurate fit to functional connectivity and irreversibility (Mueller et al., 2013). The whole-brain model adapts the strength of existing anatomical connectivity by altering conductance value parameters in order to optimize connectivity. Iterative estimation of the GEC with pseudo-gradient descent optimization allows for fitting to the empirical irreversibility covariance matrix, minimizing the mean-squared error between empirical and simulated functional connectivity matrices and the irreversibility covariance matrices. This model, in turn, allows for evaluation of the generative mechanisms creating hierarchy within conditions and, importantly, the hierarchical reconfiguration between conditions. A Hopf oscillator model was used as it has previously been shown it provides the best fit (Deco, Cruzat, Cabral, et al., 2019; Deco & Kringelbach, 2017; Deco et al., 2017; Kringelbach et al., 2023). Deviations between empirical and optimized, convergent simulated functional connectivity and respective covariance matrices are available in Supplemental Figure A.2.

The extent to which one region orchestrates the activity of others is evaluated through summation of the in-degree and out-degree across each region in the brain. As can be seen in Figure A.3, this measure of orchestration varies significantly across conditions. Under the long-term users of ayahuasca, orchestration was found to be most significant in the bilateral pre- and post-central, insula, and superior temporal, as well as the superior frontal gyrus. Under DMT, the insula was less well-connected, though bilateral precuneus became more connected. Under chronic use of cannabis, significant orchestrators were the bilateral isthmus cingulate and rostral anterior cingulate, as well as the bilateral insula. Similarly, bilateral isthmus cingulate and rostral anterior cingulate were primary orchestrators of functional organization under the occasional use of cannabis, as well as the bilateral insula. To complement the analysis of information flow between different regions captured by the GEC matrix under altered states of consciousness, we decomposed all brain regions into their canonical resting-state networks and evaluated changes between baseline or placebo and drug conditions on orchestration, characterized by the sum of the in-degree and out-degree, or incoming and outgoing information, from each network (Yeo et al., 2011). Figure A.3c details the modulation of resting-state network orchestration by ayahuasca, DMT, and cannabis.

Regional and network-level orchestration provides information about connectivity changes, but the degree to which a region orchestrates global brain activity is not directly a measure of hierarchy. To better examine the effects of chronic and occasional use of psychedelics and cannabis on the functional, hierarchical organization of the brain, we applied trophic coherence to the effective connectivity derived from the GEC, utilizing the degree of orchestration for each region. Trophic coherence, which we call directedness to differentiate from the method itself, is primarily a measure of how neatly nodes in a network fall into distinct levels, which

is analyzed by the standard deviation of the distribution of height differences along edges (S. Johnson et al., 2014; MacKay et al., 2020). The measure was first applied to ecological food webs in an attempt to better understand the stability of networks, but it can be applied to any directed network. Previously, it was used to model the coherence of social systems, including dictatorships, military regimes, and anarchy, which found that rigid, hierarchical social systems tend to have higher directedness than democracies or anarchy (Pilgrim et al., 2020). That is, a higher directedness is associated with a more rigid, stratified network structure. Here, we consider the effective connectivity of the brain as a directed network, where the degree to which a region orchestrates activity assigns it a trophic, or hierarchical, level that describes its influence over the brain. It is then possible to query the directedness of the network. Networks which display high directedness are clearly defined with regard to each nodes influence over others and are highly stratified. The corollary is that networks with low directedness are highly disordered and lack clearly defined influence relations.

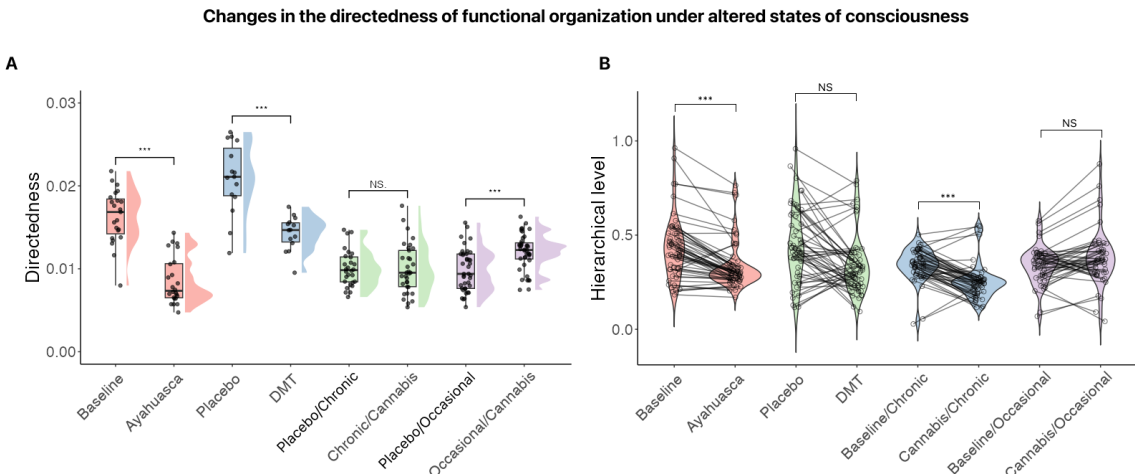


Figure 3.3: Changes in the directedness of functional organization under altered states of consciousness. (A) Changes in directedness of the effective connectivity between baseline and placebo and drug conditions. Compared with baseline, directedness under ayahuasca ( $t = -8.92$ ,  $d = 2.50 [1.73 3.26]$ ,  $p = 2.015e-11$ ) and DMT significantly decreased ( $d = 0.82 [0.10 1.54]$ ,  $p = 0.010$ ). Interestingly, baseline directedness was much higher for participants in the DMT dataset. Nonsignificant trend toward decrease was found for the chronic use of cannabis ( $p = 0.52$ ), while a significant increase in directedness was found for the occasional use of cannabis ( $Z = -3.83$ ,  $d = -0.91 [-1.36 -0.45]$ ,  $p = 1.28e-4$ ). (B) Changes in trophic levels after 10,000 iteration non-parametric permutation testing (threshold = 0.01, FDR correction threshold = 0.2). Under ayahuasca, most regions tend to decrease in hierarchical level, while both trends exist for DMT.

We first analyzed the changes in directedness of the functional organization of the brain under different states of consciousness, as well as changes in the individual trophic levels for each region in the brain from baseline or placebo to drug condition. In Figure 3.3a, it can be seen that directedness, a direct measure of hierarchical organization, significantly decreases under ayahuasca ( $t = -8.92$ ,  $d = 2.50 [1.73 3.26]$ ,  $p = 2.015e-11$ ) and DMT ( $d = 0.82 [0.10$

1.54],  $p = 0.010$ ). In contrast, the occasional use of cannabis resulted in a significant increase in the directedness of the brain's functional hierarchical organization ( $Z = -3.83$ ,  $d = -0.91$  [-1.36 -0.45],  $p = 1.28e-4$ ), while chronic use of cannabis had no effect ( $p = 0.52$ ), possibly due to tolerance (J. Ramaekers et al., 2022). Due to differences in study design, fMRI equipment, and acquisition and preprocessing techniques it is not possible to make statistical comparisons against conditions. However, we were uniquely positioned to make inferences about the nature of chronic and occasional use of psychedelics and cannabis. We also examined changes in hierarchical levels for each of 80 regions with a 10,000 iteration non-parametric permutation test, followed by a second permutation test between mean hierarchical level changes across regions between conditions. In Figure 3.3b, alterations in the hierarchical levels within regions across conditions can be seen. Alterations in directedness can be considered as a change in the variance of hierarchical levels across conditions. While directedness decreased significantly for DMT, hierarchical levels varied with regard to their change in influence. For ayahuasca and occasional use of cannabis, most levels decreased greatly, with the exception of a few at the bottom of the hierarchy. A similar pattern was seen for the chronic and occasional use of cannabis, where regions at the bottom and top of the hierarchy tended to increase in influence.

While the measure of orchestration provides a measure of the connectedness of regions, it does not *a priori* necessitate alterations in hierarchy. Trophic coherence, in contrast, provides direct access to examining alterations in the functional hierarchical organization of the brain. Figure 3.4 details the trophic levels which describe the degree of influence a brain region holds for each condition. As can be seen in Figure 3.4a, variability in trophic levels is visually distinct for the chronic and occasional use of cannabis versus ayahuasca and DMT. Considerable variability under cannabis for occasional users differs from the DMT state, whose variability is similar to ayahuasca. These results suggest that tolerance and chronicity play a different role in the changes in functional organization underlying disparate altered states of consciousness.

We examined changes from baseline or placebo for each condition through individual, 10,000 iteration non-parametric permutation tests for each region across each condition. It can be seen that unlike ayahuasca, DMT resulted in considerable increases in bilateral pre- and post-central trophic levels, as well as in the bilateral precuneus, paracentral, and isthmus cingulate (Figure 3.4b). The largest increases and decreases in trophic levels for each condition provide additional information about the nature of these altered states. Interestingly, increases in trophic levels were found for subcortical structures under ayahuasca, including the right putamen ( $P < 0.01$ , FDR corrected) and left globus pallidus externus, not rendered here ( $P < 0.01$ , FDR corrected). Decreases were seen in bilateral superior parietal, left medial orbitofrontal, left isthmus cingulate, and left posterior cingulate, consistent with previous results (R. L. Carhart-Harris et al., 2016; Timmermann et al., 2019). For DMT, increases were found in left and right pre-central, left transverse temporal, and left and right post-central ( $P < 0.01$ , FDR corrected). Under the chronic use of cannabis, decreases in trophic level were seen all across the brain, except in left and right medial and lateral occipital cortex, left and right thalamus, and right globus pallidus

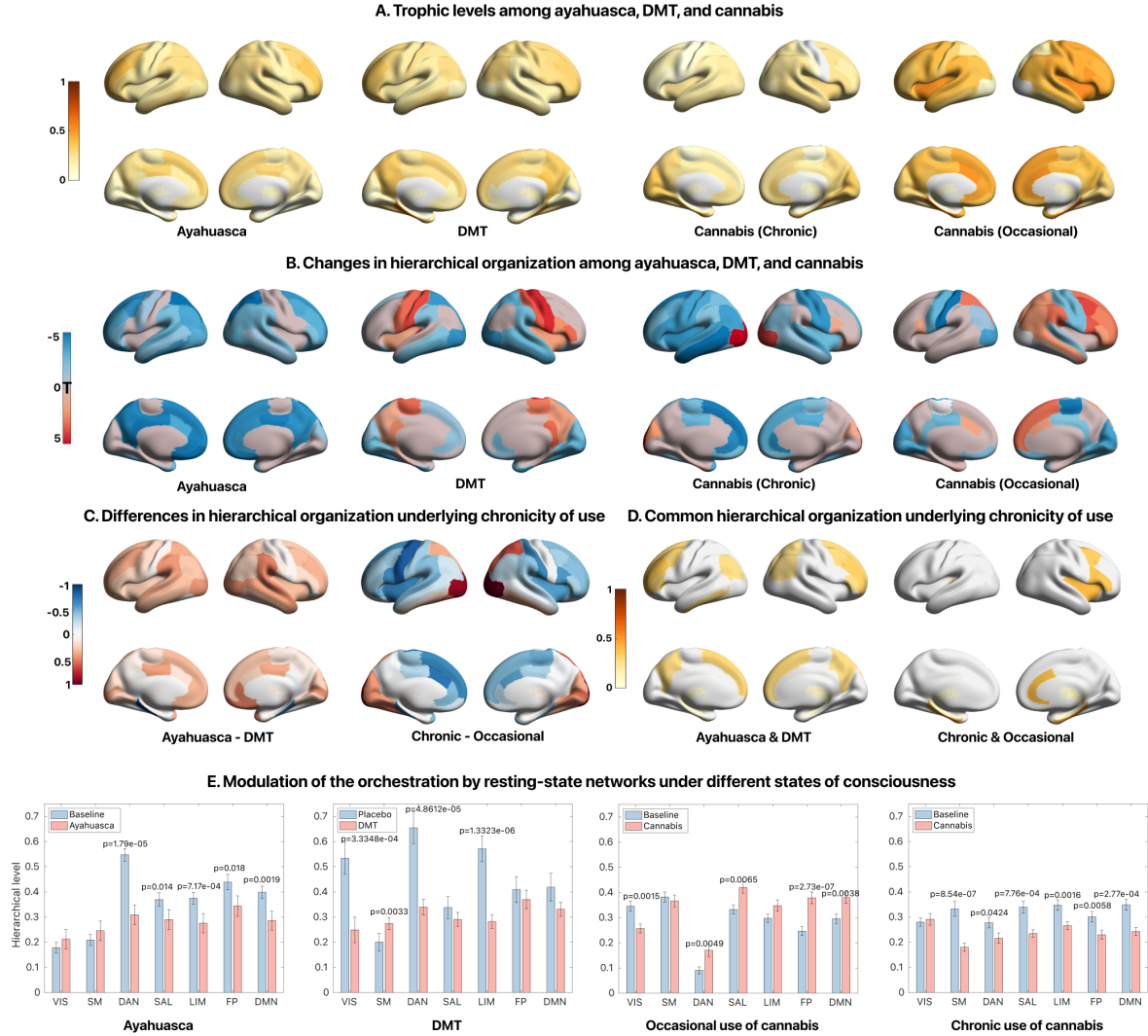


Figure 3.4: Changes in the regional hierarchy orchestrating altered states and their common hierarchical architecture. (A) Regional hierarchy in acute ayahuasca, DMT, and cannabis in chronic and occasional users. Significant variability can be seen for occasional users on cannabis, but not for ayahuasca, DMT, or cannabis in chronic users. (B) Changes in regional hierarchy from baseline or placebo to drug condition. Non-parametric 10,000 permutation testing with FDR correction identified significant regions. Non-significant regions are shaded grey. (C) Differences in regional hierarchy underlying chronicity of drug use in acute conditions. Ayahuasca resulted in generally higher regional hierarchy across the cortex than DMT. With cannabis, occasional use resulted in stronger hierarchy than in chronic use, except for the occipital cortex. (D) Common regional hierarchy underlying chronicity of drug use in acute conditions. The top 25% regions in the hierarchy were examined for each drug condition and we found the intersection between the psychedelics and between cannabis conditions.(E) Modulation of resting-state network hierarchy. Significant decreases (5,000 iteration non-parametric permutation testing, FDR corrected) were found for ayahuasca, DMT, and chronic use of cannabis. Variability in regional hierarchy was found for occasional use of cannabis.

internus ( $P < 0.01$ , FDR corrected). Decreases were found in left middle temporal, left inferior temporal cortex, left superior frontal cortex, and the left and right rostral anterior cingulate

cortices ( $P < 0.01$ , FDR corrected). For the occasional use of cannabis, increases were found in the right subthalamic nucleus, right caudal middle frontal, right pars opercularis, right supramarginal, and right superior frontal ( $P < 0.01$ , FDR corrected). Decreases in regional hierarchy were found in the right lateral occipital, left and right paracentral, left post-central, and right pericalcarine ( $P < 0.01$ , FDR corrected).

We then examined differences in regional hierarchy between acute occasional and chronic use contrasts (Figure 3.4c). Ayahuasca generally had higher regional hierarchy across the cortex than did DMT – in particular, left rostral anterior cingulate cortex and right supramarginal. For Chronic>Occasional, it was found that cannabis in occasional users induced considerably higher regional hierarchy than in chronic users, except in the medial and lateral left and right occipital cortices and superior parietal cortices. After finding differences between conditions, we sought to understand common effects of psychedelics and cannabis across the chronicity of use (Figure 3.4d). We took the top 50% of regions in the hierarchy and evaluated the intersection between them. For ayahuasca and DMT, these common influential regions were in the frontal cortex, as well as left and right superior parietal cortices, superior frontal cortices, and precuneus. For cannabis in chronic and occasional users, these common regions were the right insula, pars opercularis, pars triangularis, and caudal middle frontal, as well as the left anterior cingulate cortex.

To explore changes in the functional integrity of resting-state networks after the administration of psychedelics, we decomposed trophic levels for each region into the resting-state network most associated with that region for changes in trophic level from baseline. Figure 3.4e shows the alterations in resting-state network hierarchical influence after the administration of ayahuasca, DMT, and the chronic or occasional use of cannabis. Non-parametric, 10,000 iteration permutation-based hypothesis testing ( $\alpha = 0.01$ ) was followed by FDR correction ( $q = 0.2$ ). Significant decreases were seen for ayahuasca and DMT in the dorsal attention and limbic networks, while ayahuasca also significantly decreased the influence of the salience, frontoparietal, and default mode networks ( $P < 0.05$ , FDR corrected). DMT, on the other hand, resulted in significant decreases in the visual network and increases in the somatomotor networks ( $P < 0.05$ , FDR corrected). Similarly, occasional use of cannabis saw decreases in the visual network, but increased network hierarchy in the dorsal attention, salience, frontoparietal, and default mode networks ( $P < 0.05$ , FDR corrected). Lastly, decreases were found across all resting-state networks but the visual network for the chronic use of cannabis ( $P < 0.05$ , FDR corrected). Interestingly, ayahuasca induced a non-significant increase in both visual and somatomotor networks, consistent with the idea of a disinhibition of unimodal sensory networks under psychedelics. It is quite a surprise that the visual network hierarchy was significantly higher in resting-state than on DMT.

Developing a new framework for assessing the direct, causal interactions orchestrating changes in the functional hierarchical organization of the brain not only required the evaluation of how these measures compared with irreversibility and the measure of orchestration of the GEC, but

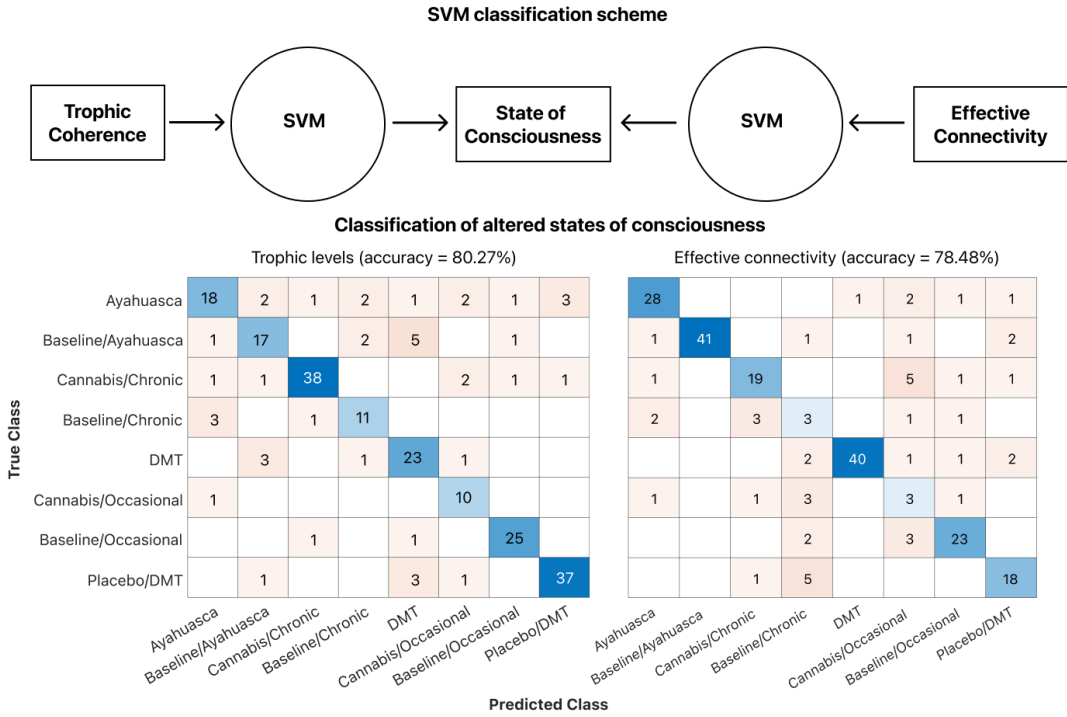


Figure 3.5: Trophic coherence is an equivalently performing, simpler discriminator of states of consciousness than effective connectivity. Figure shows the confusion matrix of the classification performance (across 5-fold k-fold cross-validation). As can be seen, the trophic coherence is an equal predictor of the conscious state condition than effective connectivity (the GEC). The average performance for trophic coherence is 80.27%, while the performance for effective connectivity is slightly lower (78.48%).

also to understand whether regional hierarchy can better discriminate between altered states of consciousness than effective connectivity alone. We fit a support vector machine (SVM) as a classifier using either the regional trophic levels or the effective connectivity matrix to classify the state of consciousness across conditions. Figure 3.5 shows the classification scheme, as well as the confusion matrix describing the accuracy of models (see Methods). It was found that regional hierarchy predicted the drug or baseline/placebo condition with 80.27% accuracy, while the effective connectivity matrix predicted the condition with 78.48% accuracy. Directedness, and the global measure of irreversibility are not suitable for this sort of classifier approach – more features are needed, which is why we use either the subjects-by-region trophic level matrix, or the region-by-by-region irreversibility matrix. In this case, the trophic levels are considered to be less rich in terms of raw data, but the classifier is able to predict equally the state with a small increase in accuracy. Regional hierarchy derived by trophic coherence thus provides a substantive and accurate dimensionality reduction of the network properties of the irreversibility matrix that captures the functional hierarchical organization of the brain.

Lastly, we endeavored to better understand the relationship between lifetime use of psychedelics, recency of use, and alterations in functional hierarchical organization. We modeled the linear relationship between the directedness of networks and lifetime use or recency

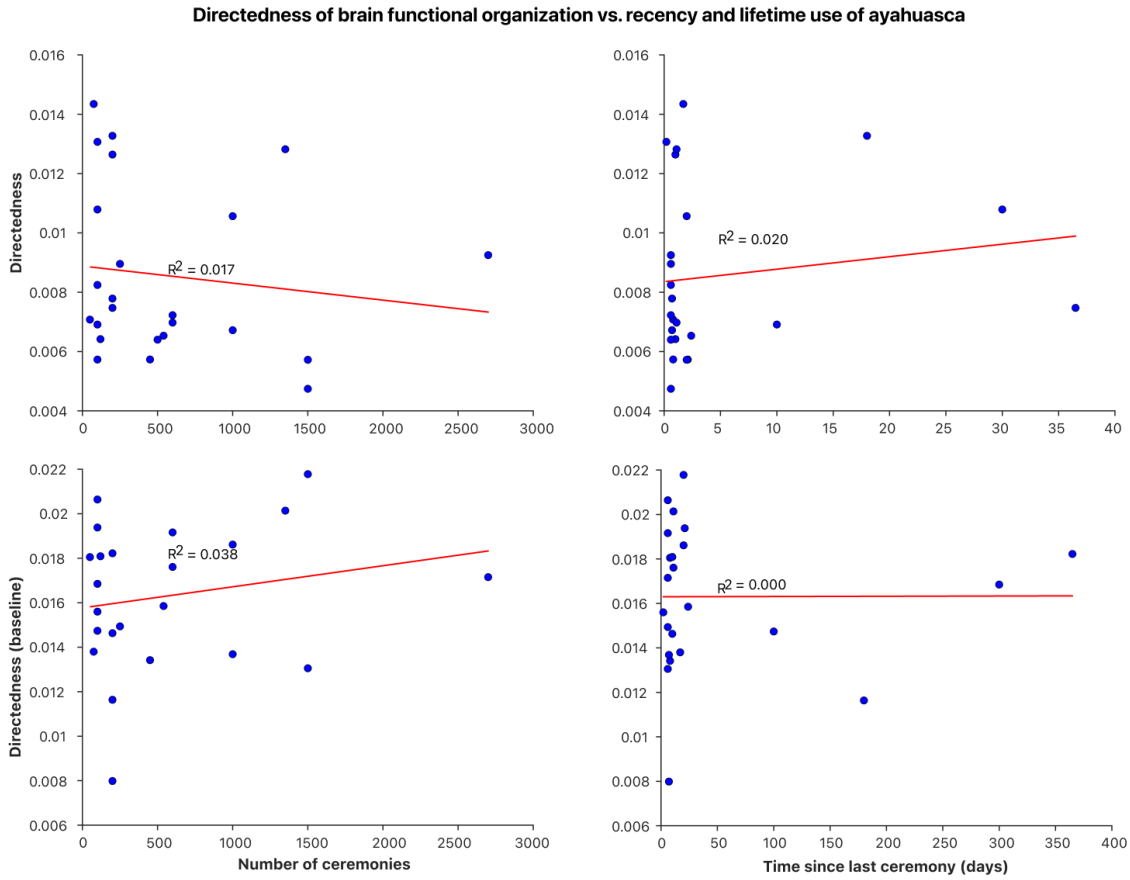


Figure 3.6: Directedness of brain functional organization vs. lifetime use of ayahuasca and recency of use. Linear mixed effect models were fit with directedness (pre- or post-ayahuasca) as the variable to be predicted, lifetime use or recency as fixed effects, and dosage as a covariate. Statistical significance was not found for any parameter. Post-ayahuasca vs number of ceremonies (top-left panel) showed a downward trend with regard to directedness, with weak correlation ( $R^2 = 0.017$ ,  $p = 0.85$ ). Post-ayahuasca vs. time since last ceremony showed an upward trend with weak correlation ( $R^2 = 0.020$ ,  $p = 0.73$ ). Baseline measures of directedness (bottom-left panel) showed opposite results against number of ceremonies, where baseline directedness tended to be higher as the total number of ceremonies for each participant increased ( $R^2 = 0.0038$ ,  $p = 0.99$ ). Baseline measures of directedness show no trend with time since last ceremony ( $R^2 = 0.000$ ,  $p = 0.37$ ).

for both baseline levels of directedness, as well as altered levels under ayahuasca. In Figure 3.6, it can be seen that there do not appear to exist any trends between these measures. Linear mixed-effect models were fit with post- or pre-ayahuasca directedness as outcome and lifetime use, in this case number of ayahuasca ceremonies, or recency of use (time since last ceremony) as fixed effects with the dosage of ayahuasca administered as a covariate. Despite regional and network-level hierarchy differences between ayahuasca and DMT, a tolerance effect over both short and long timescales does not appear to be present. It may be the case that hierarchical measures do not provide an accurate representation of changes in the brain resulting from long-term use of psychedelics.

## Discussion

Here we apply trophic coherence, a measure of the hierarchy of complex networks, to the effective connectivity derived from irreversibility across ayahuasca, DMT, and the chronic and occasional users of cannabis. These results present the use of direct measures of hierarchy on psychedelic data for the first time, and advance our understanding of how psychedelics modulate the hierarchical organization of the brain in both healthy long-term users of ayahuasca, and relatively naive users of DMT. Our main finding, that directedness decreases under both ayahuasca and DMT, is consistent with previous work showing a compression of the principal gradient of cortical hierarchy under LSD, and lends credence to a recent, unified theory of psychedelic action (R. Carhart-Harris & Friston, 2019; Girn et al., 2022).

We began with the analysis of irreversibility across conditions. We found that irreversibility decreases significantly for DMT, while a nonsignificant trend toward decreased irreversibility was found for the occasional use of cannabis – an intriguing finding, as one might intuitively expect that an effect of a drug would be nullified by tolerance effects. No trend was found for occasional use. It remains unknown whether the nonsignificant trend for ayahuasca is a result of tolerance or dosage – while users both consumed a very large amount of ayahuasca over their lifetime (mean = 564, SD = 650), they also tended to consume ~25% of the DMT that users in the DMT study consumed. This presents a limitation of the present work – while we controlled for differences in dosage within conditions, we do not make any statistical comparisons across conditions due to differences in fMRI acquisition protocol and participant demographics. With that, it was not possible to control for dosage across conditions, and it is nontrivial to make any inferences regarding between-condition effects. While it has been previously shown that irreversibility presents a more sensitive measure of states of consciousness than functional connectivity, an interpretation of what irreversibility in the human brain means is sorely needed (Deco et al., 2022; Kringelbach et al., 2023). Irreversibility is defined as the Kullback-Leibler distance between the forward and backward transition probabilities of the dynamical evolution of a system. It is therefore a measurement of the time-asymmetry of a system. This feature relates irreversibility directly to the production of entropy in a system – breaking of the detailed balance, where net fluxes between underlying states become irreversible in time, results in the production of entropy (Deco et al., 2022). According to Buzsáki (2019), the self-organized dynamics of the brain constrain how it works on the world, rather than being driven by sensations.

From this assumption, it is clear that time-asymmetric, irreversible processes would be driven by extrinsic dynamics. Though previous work by Lynn et al. (2021) has shown that entropy production in the brain increases with the physical exertion associated with a task, it also increases with cognitive exertion. Thus the association between irreversibility and hierarchy is nontrivial – it cannot be said with certainty that a change in irreversibility is associated solely with an alteration in extrinsic versus intrinsic driving of the system, or with sensitization of higher-order networks like transmodal cortex to unimodal sensory cortices.

A variety of previous work has shown that psychedelics increase entropy in the brain (Barrett et al., 2020; R. Carhart-Harris et al., 2014; Kringelbach et al., 2020; A. V. Lebedev et al., 2015; A. Lebedev et al., 2016; Luppi et al., 2023; Tagliazucchi et al., 2014; Varley et al., 2020; Viol et al., 2017), though researchers vary in a) the method used for analyzing entropy and b) the specific features of neuroimaging data they are measuring (McCulloch et al., 2022, 2023; Shinozuka et al., 2023). Here, we estimate the production of entropy, which is distinct from previous examinations of Shannon entropy or Lempel-Ziv complexity (Lempel & Ziv, 1976; Tagliazucchi et al., 2014; Ziv & Lempel, 1977). The wealth of research investigating the entropic effects of psychedelics is derived from the entropic brain hypothesis, defined by R. Carhart-Harris et al. (2014), which posits that the subjective effects of psychedelics are reflective of global increases in entropy. Interestingly, psychedelics represent the first finding of increased entropy in the human brain, whereas a decrease in entropy has previously been found for a variety of diminished or loss of consciousness states (Abásolo et al., 2015; Casali et al., 2013; Mediano et al., 2021; Zhang et al., 2001). Though the evidence across these methodologies indicates that psychedelics do, indeed, increase entropy in the brain, replication is needed to confirm this evidence. Recent efforts by McCulloch et al. (2023) have resulted in the creation of a toolbox that will allow researchers to independently replicate a wide variety of entropy metrics on their own data, which is an invaluable tool for replication of previous findings.

At the upper bound, entropy production is inverse to entropy – as entropy becomes maximized within a system, reaching an asymptotic limit, entropy production decays to zero. Importantly, entropy production is defined explicitly as the derivative of entropy, the rate at which it changes. Entropy production can be negative for microscopic systems, but due to fluctuation theorems, the probability that the reverse, entropy-producing process will occur decreases exponentially with the amount of entropy which needs to be reduced. Thus, for macroscopic systems, the probability of a decrease in entropy becomes extremely low. Furthermore, it is important to note that it is not merely by the nonequilibrium dynamics of microscopic processes that entropy is produced at larger scales. By coarse-graining a system, it is theoretically possible to average over the nonequilibrium degrees of freedom and "regain" detailed balance (Esposito, 2012; Lynn et al., 2021; Martínez et al., 2019). Irreversibility at larger scales, like those found in neural timeseries, may be emergent rather than resulting directly from nonequilibrium microscopic interactions.

It is unlikely that entropy is fully maximized within the human brain regardless of the state

of consciousness. Previous work has sought to explain an increase in entropy as reflective of criticality within the brain, a phenomena where a system is poised between 'order' and 'disorder,' such that specific features including power-law scaling and fractal self-similarity are found (Bak, 1999; R. Carhart-Harris & Friston, 2019; Petermann et al., 2009). However, an increase in entropy does not directly imply a move toward criticality. Maximization of entropy, or specifically *configurational* entropy, measuring the number of metastable states a system can take on, would imply criticality (Haldeman & Beggs, 2005). However, no studies to date have demonstrated maximization of this configurational entropy – to the contrary, previous work by Ruffini et al. (2023) who fit an Ising model to fMRI data of LSD showed that the brain operates near criticality in resting-state; LSD brought the brain away from criticality. Our results show that under both a low dose of DMT in the form of ayahuasca, and a high dose of DMT (20mg) delivered intravenously, entropy is not maximized, because irreversibility remains above zero. It may be the case that this is an error resulting from the proxy method rather than direct examination of production entropy. This may very well be the case, given that previous work by Atasoy et al. (2017) has shown elements of power-law scaling under psychedelics. Future work examining the relationship between psychedelics, entropy, and criticality should seek to use more precise measurements to analyze production entropy, though these are computationally expensive and often difficult to interpret (Deco, Perl, et al., 2021; Lynn et al., 2021; Seif et al., 2021). However, the methods described by Lynn et al. (2021) are reasonable to compute across resting-state networks and may still provide viable global measures of production entropy in the psychedelic state.

While a number of previous studies with neuroimaging data have applied graph-theoretical measures to the brain, mostly with functional connectivity (Bullmore et al., 2009; Goldenberg & Galván, 2015; Sporns & Betzel, 2016), to our knowledge this is the first time trophic coherence has been evaluated on effective connectivity data in the human brain, and a first example of measuring brain hierarchy within the context of chronicity of use of psychedelics and cannabis. Previous work by Luppi et al. (2021) utilized functional connectivity with measures including small-world propensity. Though these measure nested hierarchies, they are based on an undirected network derived from functional connectivity approaches and do not allow for causal inferences regarding directed flow of information through the brain (Reid et al., 2019). Effective connectivity offers both a way of utilizing graph-theoretical measures that are only valid on directed networks, such as trophic coherence and non-normality (Asllani et al., 2018; Pilgrim et al., 2020). Trophic coherence has been shown to be a proxy for the stability of food webs (S. Johnson et al., 2014), and the presence (or lack) of cycles within a graph is inherently linked with the directedness of that graph S. Johnson and Jones (2017). It has been closely linked with hierarchy, where a hierarchy akin to dictatorship is maximally coherent, and anarchy is maximally incoherent (Pagani et al., 2019; Pilgrim et al., 2020). These analogies work well in the present work, given the RElaxed Beliefs Under Psychedelics (REBUS) model considers the psychedelic state akin to an 'anarchic brain' – that is, decreased within-network integrity and

between-network segregation results in greater feedback between regions (R. Carhart-Harris & Friston, 2019). It is important to note that an anarchic brain state does not necessitate the total absence of hierarchy. Rather, it is assumed that metastable, quasi-hierarchical substates are traveled through over the course of the brain's trajectory (Pilgrim et al., 2020). Future work should explore the dynamics of rich club or clique generation with regard to directedness (Deco, Vidaurre, & Kringelbach, 2021; Dennis et al., 2013).

With this in mind, increased metastability may be closely linked with decreased directedness (Lord et al., 2019). Here, we found decreased directedness under ayahuasca and DMT, which provides direct evidence for the hypothesis that psychedelics induce more anarchic, or less hierarchical, brain states. Furthermore, this finding is consistent with previous work by Lord et al. (2019) indicating that the brain undergoes increased metastability under psychedelics. Previous criticism by Papo (2016) argued that the short scanning periods, especially in fMRI data, are insufficient for establishing the true number of metastable states the brain travels through. It may be the case that trophic coherence, and similar graph-theoretical measures of hierarchy, may provide a sufficient methodology for understanding criticality within fMRI research. Future research should investigate the relationship between brain hierarchy, the emergence of quasi-stable states in less hierarchical states of consciousness, and metastability. While fMRI may be insufficient for metastability analysis, modalities with higher temporal resolution that retain some of the spatial resolution of MRI, like MEG, may be a perfect fit for this line of work.

Previous work examining time to consensus in simulated social systems has shown directedness is associated with the efficiency of information transmission – the more directed a network, the faster the time to consensus (Pilgrim et al., 2020). However, our findings that cannabis increases directedness complicate this issue – it is unlikely that cannabis increases efficiency. This presents an interesting case that should be examined by future research, given that higher metastability and associated criticality are maximally efficient with regard to information transmission (Barnett et al., 2013; Shew & Plenz, 2013; Shew et al., 2009). Future research should relate local and global graph metrics, including contagion dynamics and consensus timing, to better characterize the relationship between trophic coherence and the efficiency of information transmission within brain networks.

Importantly, we apply a direct measure of hierarchy, trophic coherence, to better assess changes in the brain and empirically test the theory that psychedelics flatten brain hierarchy (R. Carhart-Harris & Friston, 2019). A recent, unified model of the action of psychedelics on the brain which combines hierarchical predictive coding with the free energy principle, 'Relaxed Beliefs Under Psychedelics' (REBUS), proposed that psychedelics induce a relaxation, or increase in sensitivity, of high-level priors, which are thought to be encoded or represented in the neural activity of transmodal association cortex (R. Carhart-Harris & Friston, 2019; K. Friston, 2010). Since publication, researchers have sought to understand how we can best empirically test this idea. Though we do not currently understand how to test directly for the relaxation of high-level priors, recent work has proposed that these priors are, in fact, encoded hierarchi-

cally within the brain (Brodski-Guerniero et al., 2017). Caucheteux et al. (2023) found, indeed, that frontoparietal cortices predicted higher-level, more contextual representations than temporal cortices. If this is the case, then direct measures of the topological hierarchy of the brain are viable for testing whether the hierarchy of the brain 'flattens' under psychedelics. Indeed, we find that directedness decreases under both ayahuasca and DMT. Interestingly, hierarchy increases in the occasional use of cannabis, but no change was found for chronic users. Similar results with complexity and entropy analysis of ketamine have been shown, indicating that ketamine, despite acting principally on the N-methyl-D-aspartate (NMDA) receptor, may act in a similar fashion with regard to hierarchical organization (Farnes et al., 2020; Roy et al., 2021; Sarasso et al., 2015; Wang et al., 2017). However, ketamine differs in that therapeutic doses increase complexity, while anesthetic doses are associated with decreased complexity. Future work should seek to examine hierarchical organization under ketamine, given that psychedelics and ketamine are thought to converge on similar signaling pathways involving neuroplasticity (Aleksandrova & Phillips, 2021). It is thus believed that psychedelics may induce a unique effect on the hierarchical organization of the brain relative to other psychoactive substances, though future work may better inform the contrast between psychedelics and other drugs. Our findings are consistent with previous work indicating a compression of the principal gradient spanning unimodal to transmodal cortex, or the bottom to top of the hierarchy, under psychedelics (Girn et al., 2022), as well as work by Singleton et al. (2022) indicating that psychedelics flatten the control energy landscape of the brain, allowing more facile state transitions. While the latter is not a measure of hierarchy *per se*, it is consistent with the idea of quasi-stable hierarchies within the broader, 'anarchic' network under psychedelics.

We propose that the flattening of brain hierarchy under psychedelics occurs at a global level over the course of a psychedelic experience, but that quasi-stable hierarchical structures emerge over shorter timescales and in lower-order spaces of the whole brain network. The use of dynamic approaches to whole-brain modeling allows for analysis of dynamic alterations in global hierarchical structures over the scanning period (Bahrami et al., 2022; Deco & Kringelbach, 2014). Previous research with dynamic functional connectivity and leading eigenvector dynamics analysis (LEiDA) allowed for characterization of metastable substates within the psychedelic experience that, with whole-brain modeling, allows for characterization not only of dynamical substates, but of directed network effects including stability, consensus timing, and the reconfiguration of directedness and trophic levels (Cabral et al., 2017; Lord et al., 2019).

Lastly, we performed an exploratory analysis of the chronic effects of psychedelics, contrasting them with the well-defined characteristics of the tolerance effects induced by cannabis. We find that psychedelics differ greatly, in that patterns of alterations in irreversibility are opposed for psychedelics relative to cannabis. We find that irreversibility does not significantly decrease for ayahuasca, but that it does for DMT, an effect we cannot disentangle from differences in dosage. Irreversibility decreases for occasional users of cannabis but not for chronic users, indicating that some element of tolerance or chronicity may be present under both psychedelics

and cannabis. This effect is made more nuanced by our measure of directedness, where both ayahuasca and DMT show decreases in directedness, but increases are found for occasional users and no significant effect is found for chronic users of cannabis. These results distinguish that under both lower doses and higher doses of DMT itself, changes in hierarchy are found, and argue against the notion that lifetime use or recency of use of psychedelics has any meaningful relationship to effects in response to psychedelics. Though we cannot compare directly, it is notable that baseline and placebo conditions for ayahuasca and DMT differ in their directedness, where ayahuasca users generally had lower directedness at baseline than users of DMT. Further research should seek to compare long-term users of psychedelics with naive users in a controlled setting, matching for age and sex if possible, and using the same acquisition and recruitment protocols.

Though structural changes have been found in the morphology of long-term users of ayahuasca (Bouso et al., 2015), we do not find here any opposing results with regard to irreversibility across the brain or brain hierarchy. With regard to the hierarchical levels of each region in the brain, we saw a notable difference between ayahuasca and DMT in that levels decreased significantly for ayahuasca, with a few notable exceptions at the bottom of the hierarchy moving up in influence. In contrast, no significant effect was found for DMT – this is likely to be because of the high variability in whether a region increased in influence or decreased. This differential effect between ayahuasca and DMT is likely then to result from either chronicity of use, differences in dose, or possibly the inclusion of a monoamine oxidase inhibitor (MAOI) in the preparation of DMT. Future work should seek to compare DMT administration directly in both conditions with the same dosage in order to isolate the effects of chronicity.

We noticed significant changes in hierarchical influence of resting-state networks between conditions. Ayahuasca resulted in significant decreases in hierarchy of the dorsal attention network, salience network, limbic network, frontoparietal network, and default mode network, while the same networks were only significantly modulated under DMT in the dorsal attention and limbic networks. A similar trend was seen for all networks between ayahuasca and DMT, except in the visual network, which saw a strong, significant decrease for DMT but a small, nonsignificant increase for ayahuasca. It is difficult to interpret these changes between psychedelics and cannabis, but generally we found increases in resting-state network influence for all but visual network under occasional use, and decreases for the chronic use of cannabis. This differential regulation of resting-state networks is easier to isolate, given that the dosage and acquisition protocol were identical across chronic and occasional conditions. These results, then, provide further evidence toward the chronic effects of cannabis, indicating that chronic use reverses response patterns to cannabis with regard to hierarchy. Previous work has largely focused on neuromodulation at the cellular and molecular level (Bosker et al., 2013; Hirvonen et al., 2012), though some work into fingerprints of occasional and cannabis use has been performed, which is the primary study predating our analysis of this data (J. Ramaekers et al., 2022). J. G. Ramaekers et al. (2020) found that tolerance to cannabis occurs rapidly, and the effect is

maintained with continued use. Chronic effects of cannabis are highly reversible, though, which we did not think would be the case with psychedelics.

Given the heterogeneity of lifetime use and recency of use within the ayahuasca group, we decided to analyze brain hierarchy in both baseline and psychedelic conditions against this demographic data. Interestingly, we find no significant effect of recency of use or number of ceremonies on either baseline hierarchy or under ayahuasca. This provides evidence that long-term use of psychedelics does not have significant effects on the functional hierarchical organization of the brain in the long-term. It is, however, unlikely that the sample sizes here are sufficient enough to detect a robust statistical relationship between these phenomena. These results lie in contrast to recent work in patients with treatment-resistant depression, where changes in network cartography were found three weeks after the administration of psilocybin, but not escitalopram (Daws et al., 2022). The contrasting results here suggest that psychedelics may modulate network structure and hierarchical organization in the long-term in patients with mental health conditions, but not in healthy volunteers. Psychedelics, then, would be considered as 'adaptogenic,' a term typically used to describe the pharmacology of alternative medicines that argues the principal action of some psychoactive substances is to normalize, or balance, brain activity, cognition, and emotion.

Previous work in complexity and entropy has focused on advancing methodologies in order to develop more sensitive measures of states of consciousness. First work in this area by Casali et al. (2013) showed that transcranial magnetic stimulation combined with Lempel-Ziv complexity analysis in patients with disorders of consciousness was an extremely sensitive measure differentiating between states like vegetative, unresponsive wakefulness, and minimally conscious states. Recent work by Kringelbach et al. (2023) and Tewarie et al. (2023) has shown irreversibility to be a superior measure to functional connectivity in differentiating between brain states in fMRI and MEG data. Here, we show trophic coherence, which in this context effectively constitutes a dimensionality reduction of the effective connectivity of irreversibility, performs equally well as effective connectivity of irreversibility in differentiating between brain states. Interestingly, we show that a hyperparameter-optimized SVM discriminates not only between drug and placebo conditions, but between ayahuasca and DMT, chronic and occasional use of cannabis, and the respective baseline states for each condition. All data was normalized prior to model fitting, which eliminates any opportunity for the classifier to exploit differences in the arbitrary bounds of hierarchical levels within conditions. Though trophic coherence remains more computationally expensive than model-free irreversibility for the purpose of classifying states of consciousness, we maintain that the method well characterizes a unique feature, brain hierarchy, of otherwise highly-noisy neural activity.

In this study, we determined alterations in irreversibility and brain hierarchy through model-free and whole brain modelling-based analysis of the directed networks underpinning alterations in directedness under the chronic and naive use of psychedelics, and the chronic and occasional use of cannabis. Due to limitations of the design, we are not able to make statistical comparisons

across groups. However, the results are compelling and provide first evidence that the functional effects of the long-term use of psychedelics are distinct from cannabis. Furthermore, we provide direct evidence that the hierarchy of the brain is reduced under psychedelics, lending support to the REBUS model. Future research should seek to directly examine the chronic effects of psychedelic use on functional brain dynamics and hierarchy, though additional data is required to understand this. Given the rapid rate at which psychedelics are being administered to patients, and with ongoing clinical trials into the effects of psychedelics for the treatment of psychiatric illnesses, understanding the chronic effects of psychedelics is paramount to both understanding how these substances can treat mental health conditions, as well as establishing their safety and efficacy.

## References

- Abásolo, D., Simons, S., Morgado da Silva, R., Tononi, G., & Vyazovskiy, V. V. (2015). Lempel-Ziv complexity of cortical activity during sleep and waking in rats. *Journal of Neurophysiology*, 113(7), 2742–2752. <https://doi.org/10.1152/jn.00575.2014>
- Aleksandrova, L. R., & Phillips, A. G. (2021). Neuroplasticity as a convergent mechanism of ketamine and classical psychedelics. *Trends in Pharmacological Sciences*, 42(11), 929–942. <https://doi.org/10.1016/j.tips.2021.08.003>
- Andersson, J. L., Hutton, C., Ashburner, J., Turner, R., & Friston, K. (2001). Modeling geometric deformations in EPI time series. *NeuroImage*, 13(5), 903–919. <https://doi.org/10.1006/nimg.2001.0746>
- Ashburner, J. (2007). A fast diffeomorphic image registration algorithm. *NeuroImage*, 38(1), 95–113. <https://doi.org/10.1016/j.neuroimage.2007.07.007>
- Ashburner, J., & Friston, K. J. (2005). Unified segmentation. *NeuroImage*, 26(3), 839–851. <https://doi.org/10.1016/j.neuroimage.2005.02.018>
- Asllani, M., Lambiotte, R., & Carletti, T. (2018). Structure and dynamical behavior of non-normal networks. *Science Advances*, 4(12), eaau9403. <https://doi.org/10.1126/sciadv.aau9403>
- Atasoy, S., Roseman, L., Kaelen, M., Kringelbach, M. L., Deco, G., & Carhart-Harris, R. L. (2017). Connectome-harmonic decomposition of human brain activity reveals dynamical repertoire re-organization under LSD. *Scientific Reports*, 7(1), 17661. <https://doi.org/10.1038/s41598-017-17546-0>  
QID: Q47134467.
- Bahrami, M., Laurienti, P. J., Shappell, H. M., Dagenbach, D., & Simpson, S. L. (2022). A mixed-modeling framework for whole-brain dynamic network analysis. *Network Neuroscience*, 6(2), 591–613. [https://doi.org/10.1162/netn\\_a\\_00238](https://doi.org/10.1162/netn_a_00238)
- Bak, P. (1999). *How nature works: The science of self-organized criticality* (1., softcover pr.). Copernicus.
- Barbosa, P. C. R., Cazorla, I. M., Giglio, J. S., & Strassman, R. (2009). A six-month prospective evaluation of personality traits, psychiatric symptoms and quality of life in ayahuasca-naïve subjects. *Journal of Psychoactive Drugs*, 41(3), 205–212. <https://doi.org/10.1080/02791072.2009.10400530>

- Barnett, L., Lizier, J. T., Harré, M., Seth, A. K., & Bossomaier, T. (2013). Information Flow in a Kinetic Ising Model Peaks in the Disordered Phase. *Physical Review Letters*, 111(17), 177203. <https://doi.org/10.1103/PhysRevLett.111.177203>
- Barrett, F. S., Doss, M. K., Sepeda, N. D., Pekar, J. J., & Griffiths, R. R. (2020). Emotions and brain function are altered up to one month after a single high dose of psilocybin. *Scientific Reports*, 10(1), 2214. <https://doi.org/10.1038/s41598-020-59282-y>
- Beggs, J. M., & Plenz, D. (2003). Neuronal avalanches in neocortical circuits. *The Journal of Neuroscience: The Official Journal of the Society for Neuroscience*, 23(35), 11167–11177. <https://doi.org/10.1523/JNEUROSCI.23-35-11167.2003>
- Behzadi, Y., Restom, K., Liau, J., & Liu, T. T. (2007). A component based noise correction method (CompCor) for BOLD and perfusion based fMRI. *NeuroImage*, 37(1), 90–101. <https://doi.org/10.1016/j.neuroimage.2007.04.042>
- Benjamini, Y., & Hochberg, Y. (1995). Controlling the False Discovery Rate: A Practical and Powerful Approach to Multiple Testing. *Journal of the Royal Statistical Society: Series B (Methodological)*, 57(1), 289–300. <https://doi.org/10.1111/j.2517-6161.1995.tb02031.x>
- Bogenschutz, M. P., Forcehimes, A. A., Pommy, J. A., Wilcox, C. E., Barbosa, P. C. R., & Strassman, R. J. (2015). Psilocybin-assisted treatment for alcohol dependence: A proof-of-concept study. *Journal of Psychopharmacology (Oxford, England)*, 29(3), 289–299. <https://doi.org/10.1177/0269881114565144>
- Bosker, W. M., Karschner, E. L., Lee, D., Goodwin, R. S., Hirvonen, J., Innis, R. B., Theunissen, E. L., Kuypers, K. P. C., Huestis, M. A., & Ramaekers, J. G. (2013). Psychomotor function in chronic daily Cannabis smokers during sustained abstinence. *PloS One*, 8(1), e53127. <https://doi.org/10.1371/journal.pone.0053127>
- Bouso, J. C., Palhano-Fontes, F., Rodríguez-Fornells, A., Ribeiro, S., Sanches, R. F., de Souza Crippa, J. A., Hallak, J. E. C., de Araújo, D. B., & Riba, J. (2015). Long-term use of psychedelic drugs is associated with differences in brain structure and personality in humans \$. *European Neuropsychopharmacology*, 25(4), 483–492. <https://doi.org/10.1016/j.euroneuro.2015.01.008>  
MAG ID: 1972616052.
- Branchi, I. (2011). The double edged sword of neural plasticity: Increasing serotonin levels leads to both greater vulnerability to depression and improved capacity to recover. *Psychoneuroendocrinology*, 36(3), 339–351. <https://doi.org/10.1016/j.psyneuen.2010.08.011>
- Brodski-Guerniero, A., Paasch, G.-F., Wollstadt, P., Özdemir, I., Lizier, J. T., & Wibral, M. (2017). Information-Theoretic Evidence for Predictive Coding in the Face-Processing System. *The Journal of Neuroscience*, 37(34), 8273–8283. <https://doi.org/10.1523/JNEUROSCI.0614-17.2017>
- Buckner, R. L., Andrews-Hanna, J. R., & Schacter, D. L. (2008). *The Brain's Default Network: Anatomy, Function, and Relevance to Disease*. *Annals of the New York Academy of Sciences*, 1124(1), 1–38. <https://doi.org/10.1196/annals.1440.011>

- Bullmore, E., Barnes, A., Bassett, D. S., Fornito, A., Kitzbichler, M., Meunier, D., & Suckling, J. (2009). Generic aspects of complexity in brain imaging data and other biological systems. *NeuroImage*, 47(3), 1125–1134. <https://doi.org/10.1016/j.neuroimage.2009.05.032>
- Buzsáki, G. (2019). *The Brain From Inside Out*. <https://academic.oup.com/book/35081>
- Cabral, J., Vidaurre, D., Marques, P., Magalhães, R., Silva Moreira, P., Miguel Soares, J., Deco, G., Sousa, N., & Kringelbach, M. L. (2017). Cognitive performance in healthy older adults relates to spontaneous switching between states of functional connectivity during rest. *Scientific Reports*, 7(1), 5135. <https://doi.org/10.1038/s41598-017-05425-7>
- Calhoun, V. D., Wager, T. D., Krishnan, A., Rosch, K. S., Seymour, K. E., Nebel, M. B., Mostofsky, S. H., Nyakas, P., & Kiehl, K. (2017). The impact of T1 versus EPI spatial normalization templates for fMRI data analyses. *Human Brain Mapping*, 38(11), 5331–5342. <https://doi.org/10.1002/hbm.23737>
- Capouskova, K., Kringelbach, M. L., & Deco, G. (2022). Modes of cognition: Evidence from metastable brain dynamics. *NeuroImage*, 260, 119489. <https://doi.org/10.1016/j.neuroimage.2022.119489>
- Carhart-Harris, R. L., Bolstridge, M., Day, C. M. J., Rucker, J., Watts, R., Erritzoe, D. E., Kaelen, M., Giribaldi, B., Bloomfield, M., Pilling, S., Rickard, J. A., Forbes, B., Feilding, A., Taylor, D., Curran, H. V., & Nutt, D. J. (2018). Psilocybin with psychological support for treatment-resistant depression: Six-month follow-up. *Psychopharmacology*, 235(2), 399–408. <https://doi.org/10.1007/s00213-017-4771-x>
- Carhart-Harris, R. (2007). Waves of the Unconscious: The Neurophysiology of Dreamlike Phenomena and Its Implications for the Psychodynamic Model of the Mind. *Neuropsychoanalysis*, 9(2), 183–211. <https://doi.org/10.1080/15294145.2007.10773557>
- Carhart-Harris, R., Erritzoe, D., Haijen, E., Kaelen, M., & Watts, R. (2018). Psychedelics and connectedness. *Psychopharmacology*, 235(2), 547–550. <https://doi.org/10.1007/s00213-017-4701-y>
- Carhart-Harris, R., & Friston, K. J. (2019). REBUS and the Anarchic Brain: Toward a Unified Model of the Brain Action of Psychedelics (E. L. Barker, Ed.). *Pharmacological Reviews*, 71(3), 316–344. <https://doi.org/10.1124/pr.118.017160>
- Carhart-Harris, R., Giribaldi, B., Watts, R., Baker-Jones, M., Murphy-Beiner, A., Murphy, R., Martell, J., Blemings, A., Erritzoe, D., & Nutt, D. J. (2021). Trial of Psilocybin versus Escitalopram for Depression. *The New England Journal of Medicine*, 384(15), 1402–1411. <https://doi.org/10.1056/NEJMoa2032994>
- Carhart-Harris, R., Leech, R., Hellyer, P., Shanahan, M., Feilding, A., Tagliazucchi, E., Chialvo, D., & Nutt, D. (2014). The entropic brain: A theory of conscious states informed by neuroimaging research with psychedelic drugs. *Frontiers in Human Neuroscience*, 8. Retrieved April 6, 2023, from <https://www.frontiersin.org/articles/10.3389/fnhum.2014.00020>

- Carhart-Harris, R., & Nutt, D. J. (2017). Serotonin and brain function: A tale of two receptors. *Journal of Psychopharmacology*, 31(9), 1091–1120. <https://doi.org/10.1177/0269881117725915>
- Carhart-Harris, R. L. (2019). How do psychedelics work? *Current Opinion in Psychiatry*, 32(1), 16–21. <https://doi.org/10.1097/YCO.0000000000000467>
- Carhart-Harris, R. L., Erritzoe, D., Williams, T., Stone, J. M., Reed, L. J., Colasanti, A., Tyacke, R. J., Leech, R., Malizia, A. L., Murphy, K., Hobden, P., Evans, J., Feilding, A., Wise, R. G., & Nutt, D. J. (2012). Neural correlates of the psychedelic state as determined by fMRI studies with psilocybin. *Proceedings of the National Academy of Sciences of the United States of America*, 109(6), 2138–2143. <https://doi.org/10.1073/pnas.1119598109>
- Carhart-Harris, R. L., Muthukumaraswamy, S., Roseman, L., Kaelen, M., Droog, W., Murphy, K., Tagliazucchi, E., Schenberg, E. E., Nest, T., Orban, C., Leech, R., Williams, L. T., Williams, T. M., Bolstridge, M., Sessa, B., McGonigle, J., Sereno, M. I., Nichols, D., Hellyer, P. J., ... Nutt, D. J. (2016). Neural correlates of the LSD experience revealed by multimodal neuroimaging. *Proceedings of the National Academy of Sciences of the United States of America*, 113(17), 4853–4858. <https://doi.org/10.1073/pnas.1518377113>
- Carhart-Harris, R. L., Roseman, L., Bolstridge, M., Demetriou, L., Pannekoek, J. N., Wall, M. B., Tanner, M. A., Kaelen, M., McGonigle, J., Murphy, K., Leech, R., Curran, H. V., & Nutt, D. J. (2017). Psilocybin for treatment-resistant depression: fMRI-measured brain mechanisms. *Scientific Reports*, 7(1). <https://doi.org/10.1038/s41598-017-13282-7>
- Casali, A. G., Gosseries, O., Rosanova, M., Boly, M., Sarasso, S., Casali, K. R., Casarotto, S., Bruno, M.-A., Laureys, S., Tononi, G., & Massimini, M. (2013). A theoretically based index of consciousness independent of sensory processing and behavior. *Science Translational Medicine*, 5(198), 198ra105. <https://doi.org/10.1126/scitranslmed.3006294>
- Caucheteux, C., Gramfort, A., & King, J.-R. (2023). Evidence of a predictive coding hierarchy in the human brain listening to speech. *Nature Human Behaviour*, 7(3), 430–441. <https://doi.org/10.1038/s41562-022-01516-2>
- Chai, X. J., Castañón, A. N., Ongür, D., & Whitfield-Gabrieli, S. (2012). Anticorrelations in resting state networks without global signal regression. *NeuroImage*, 59(2), 1420–1428. <https://doi.org/10.1016/j.neuroimage.2011.08.048>
- Constantin, A.-E., & Patil, I. (2021). ggsignif: R package for displaying significance brackets for 'ggplot2'. *PsyArxiv*. <https://doi.org/10.31234/osf.io/7awm6>
- Davis, A. K., Barrett, F. S., May, D. G., Cosimano, M. P., Sepeda, N. D., Johnson, M. W., Finan, P. H., & Griffiths, R. R. (2021). Effects of Psilocybin-Assisted Therapy on Major Depressive Disorder: A Randomized Clinical Trial. *JAMA psychiatry*, 78(5), 481–489. <https://doi.org/10.1001/jamapsychiatry.2020.3285>
- Daws, R. E., Timmermann, C., Giribaldi, B., Sexton, J. D., Wall, M. B., Erritzoe, D., Roseman, L., Nutt, D., & Carhart-Harris, R. (2022). Increased global integration in the brain after

- psilocybin therapy for depression. *Nature Medicine*, 28(4), 844–851. <https://doi.org/10.1038/s41591-022-01744-z>
- Deco, G., Cabral, J., Woolrich, M. W., Stevner, A. B. A., van Hartevelt, T. J., & Kringelbach, M. L. (2017). Single or multiple frequency generators in on-going brain activity: A mechanistic whole-brain model of empirical MEG data. *NeuroImage*, 152, 538–550. <https://doi.org/10.1016/j.neuroimage.2017.03.023>
- Deco, G., Cruzat, J., Cabral, J., Tagliazucchi, E., Laufs, H., Logothetis, N. K., & Kringelbach, M. L. (2019). Awakening: Predicting external stimulation to force transitions between different brain states. *Proceedings of the National Academy of Sciences*, 116(36), 18088–18097. <https://doi.org/10.1073/pnas.1905534116>
- Deco, G., Cruzat, J., & Kringelbach, M. L. (2019). Brain songs framework used for discovering the relevant timescale of the human brain. *Nature Communications*, 10(1), 583. <https://doi.org/10.1038/s41467-018-08186-7>
- Deco, G., & Kringelbach, M. L. (2014). Great Expectations: Using Whole-Brain Computational Connectomics for Understanding Neuropsychiatric Disorders. *Neuron*, 84(5), 892–905. <https://doi.org/10.1016/j.neuron.2014.08.034>
- Deco, G., & Kringelbach, M. L. (2017). Hierarchy of Information Processing in the Brain: A Novel ‘Intrinsic Ignition’ Framework. *Neuron*, 94(5), 961–968. <https://doi.org/10.1016/j.neuron.2017.03.028>
- Deco, G., Perl, Y. S., Sitt, J. D., Tagliazucchi, E., & Kringelbach, M. L. (2021, July 4). *Deep learning the arrow of time in brain activity: Characterising brain-environment behavioural interactions in health and disease*. <https://doi.org/10.1101/2021.07.02.450899>
- Deco, G., Sanz Perl, Y., Bocaccio, H., Tagliazucchi, E., & Kringelbach, M. L. (2022). The INSIDEOUT framework provides precise signatures of the balance of intrinsic and extrinsic dynamics in brain states. *Communications Biology*, 5(1), 1–13. <https://doi.org/10.1038/s42003-022-03505-7>
- Deco, G., Vidaurre, D., & Kringelbach, M. L. (2021). Revisiting the global workspace orchestrating the hierarchical organization of the human brain. *Nature Human Behaviour*, 5(4), 497–511. <https://doi.org/10.1038/s41562-020-01003-6>
- Dennis, E. L., Jahanshad, N., Toga, A. W., McMahon, K. L., de Zubicaray, G. I., Hickie, I., Wright, M. J., & Thompson, P. M. (2013). DEVELOPMENT OF THE “RICH CLUB” IN BRAIN CONNECTIVITY NETWORKS FROM 438 ADOLESCENTS & ADULTS AGED 12 TO 30. *Proceedings / IEEE International Symposium on Biomedical Imaging: from nano to macro. IEEE International Symposium on Biomedical Imaging*, 624–627. <https://doi.org/10.1109/ISBI.2013.6556552>
- Desikan, R. S., Ségonne, F., Fischl, B., Quinn, B. T., Dickerson, B. C., Blacker, D., Buckner, R. L., Dale, A. M., Maguire, R. P., Hyman, B. T., Albert, M. S., & Killiany, R. J. (2006). An automated labeling system for subdividing the human cerebral cortex on MRI scans

- into gyral based regions of interest. *NeuroImage*, 31(3), 968–980. <https://doi.org/10.1016/j.neuroimage.2006.01.021>
- D’Souza, D. C., Syed, S. A., Flynn, L. T., Safi-Aghdam, H., Cozzi, N. V., & Ranganathan, M. (2022). Exploratory study of the dose-related safety, tolerability, and efficacy of dimethyltryptamine (DMT) in healthy volunteers and major depressive disorder. *Neuropsychopharmacology: Official Publication of the American College of Neuropsychopharmacology*, 47(10), 1854–1862. <https://doi.org/10.1038/s41386-022-01344-y>
- Esposito, M. (2012). Stochastic thermodynamics under coarse graining. *Physical Review E*, 85(4), 041125. <https://doi.org/10.1103/PhysRevE.85.041125>
- Farnes, N., Juel, B. E., Nilsen, A. S., Romundstad, L. G., & Storm, J. F. (2020). Increased signal diversity/complexity of spontaneous EEG, but not evoked EEG responses, in ketamine-induced psychedelic state in humans. *PLOS ONE*, 15(11), e0242056. <https://doi.org/10.1371/journal.pone.0242056>
- Friston, K. J., Harrison, L., & Penny, W. (2003). Dynamic causal modelling. *NeuroImage*, 19(4), 1273–1302. [https://doi.org/10.1016/S1053-8119\(03\)00202-7](https://doi.org/10.1016/S1053-8119(03)00202-7)
- Friston, K. J., Williams, S., Howard, R., Frackowiak, R. S., & Turner, R. (1996). Movement-related effects in fMRI time-series. *Magnetic Resonance in Medicine*, 35(3), 346–355. <https://doi.org/10.1002/mrm.1910350312>
- Friston, K. (2010). The free-energy principle: A unified brain theory? *Nature Reviews Neuroscience*, 11(2), 127–138. <https://doi.org/10.1038/nrn2787>
- Friston, Karl. J., Ashburner, J., Frith, C. D., Poline, J.-B., Heather, J. D., & Frackowiak, R. S. J. (1995). Spatial registration and normalization of images. *Human Brain Mapping*, 3(3), 165–189. <https://doi.org/10.1002/hbm.460030303>
- Gasser, P., Holstein, D., Michel, Y., Doblin, R., Yazari-Klosinski, B., Passie, T., & Brenneisen, R. (2014). Safety and efficacy of lysergic acid diethylamide-assisted psychotherapy for anxiety associated with life-threatening diseases. *The Journal of Nervous and Mental Disease*, 202(7), 513–520. <https://doi.org/10.1097/NMD.0000000000000113>
- Girn, M., Rosas, F. E., Daws, R. E., Gallen, C. L., Gazzaley, A., & Carhart-Harris, R. L. (2023). A complex systems perspective on psychedelic brain action. *Trends in Cognitive Sciences*, 27(5), 433–445. <https://doi.org/10.1016/j.tics.2023.01.003>
- Girn, M., Roseman, L., Bernhardt, B., Smallwood, J., Carhart-Harris, R., & Nathan Spreng, R. (2022). Serotonergic psychedelic drugs LSD and psilocybin reduce the hierarchical differentiation of unimodal and transmodal cortex. *NeuroImage*, 256, 119220. <https://doi.org/10.1016/j.neuroimage.2022.119220>
- Goldenberg, D., & Galván, A. (2015). The use of functional and effective connectivity techniques to understand the developing brain. *Developmental Cognitive Neuroscience*, 12, 155–164. <https://doi.org/10.1016/j.dcn.2015.01.011>

- Golesorkhi, M., Gomez-Pilar, J., Zilio, F., Berberian, N., Wolff, A., Yagoub, M. C. E., & Northoff, G. (2021). The brain and its time: Intrinsic neural timescales are key for input processing. *Communications Biology*, 4(1), 1–16. <https://doi.org/10.1038/s42003-021-02483-6>
- Gomes, M. T., Fernandes, H. M., & Cabral, J. (2020, December 7). Deep brain stimulation modulates the dynamics of resting-state networks in patients with Parkinson's Disease. <https://doi.org/10.1101/2020.11.04.368274>
- Goodwin, G. M., Aaronson, S. T., Alvarez, O., Arden, P. C., Baker, A., Bennett, J. C., Bird, C., Blom, R. E., Brennan, C., Brusch, D., Burke, L., Campbell-Coker, K., Carhart-Harris, R., Cattell, J., Daniel, A., DeBattista, C., Dunlop, B. W., Eisen, K., Feifel, D., ... Malievskaia, E. (2022). Single-Dose Psilocybin for a Treatment-Resistant Episode of Major Depression. *New England Journal of Medicine*, 387(18), 1637–1648. <https://doi.org/10.1056/NEJMoa2206443>
- Griffiths, R. R., Johnson, M. W., Carducci, M. A., Umbricht, A., Richards, W. A., Richards, B. D., Cosimano, M. P., & Klinedinst, M. A. (2016). Psilocybin produces substantial and sustained decreases in depression and anxiety in patients with life-threatening cancer: A randomized double-blind trial. *Journal of Psychopharmacology (Oxford, England)*, 30(12), 1181–1197. <https://doi.org/10.1177/0269881116675513>
- Griffiths, R. R., Johnson, M. W., Richards, W. A., Richards, B. D., McCann, U., & Jesse, R. (2011). Psilocybin occasioned mystical-type experiences: Immediate and persisting dose-related effects. *Psychopharmacology*, 218(4), 649–665. <https://doi.org/10.1007/s00213-011-2358-5>
- Griffiths, R. R., Richards, W. A., Johnson, M. W., McCann, U. D., & Jesse, R. (2008). Mystical-type experiences occasioned by psilocybin mediate the attribution of personal meaning and spiritual significance 14 months later. *Journal of Psychopharmacology*, 22(6), 621–632. <https://doi.org/10.1177/0269881108094300>
- Grob, C. S., Danforth, A. L., Chopra, G. S., Hagerty, M., McKay, C. R., Halberstadt, A. L., & Greer, G. R. (2011). Pilot study of psilocybin treatment for anxiety in patients with advanced-stage cancer. *Archives of General Psychiatry*, 68(1), 71–78. <https://doi.org/10.1001/archgenpsychiatry.2010.116>
- Haldeman, C., & Beggs, J. M. (2005). Critical Branching Captures Activity in Living Neural Networks and Maximizes the Number of Metastable States. *Physical Review Letters*, 94(5), 058101. <https://doi.org/10.1103/PhysRevLett.94.058101>
- Hallquist, M. N., Hwang, K., & Luna, B. (2013). The Nuisance of Nuisance Regression: Spectral Misspecification in a Common Approach to Resting-State fMRI Preprocessing Reintroduces Noise and Obscures Functional Connectivity. *NeuroImage*, 0, 208–225. <https://doi.org/10.1016/j.neuroimage.2013.05.116>
- Henson, R., Buechel, C., Josephs, O., & Friston, K. J. (1999). The slice-timing problem in event-related fMRI. *NeuroImage*. Retrieved May 21, 2023, from <https://www.semanticscholar.org>.

- org/paper/The - slice - timing - problem - in - event - related - fMRI - Henson - Buechel / e257acebf8bbda0811d452b277208797c4b12506
- Hirvonen, J., Goodwin, R. S., Li, C.-T., Terry, G. E., Zoghbi, S. S., Morse, C., Pike, V. W., Volkow, N. D., Huestis, M. A., & Innis, R. B. (2012). Reversible and regionally selective downregulation of brain cannabinoid CB1 receptors in chronic daily cannabis smokers. *Molecular Psychiatry*, 17(6), 642–649. <https://doi.org/10.1038/mp.2011.82>
- Johnson, M. W., & Griffiths, R. R. (2017). Potential Therapeutic Effects of Psilocybin. *Neurotherapeutics: The Journal of the American Society for Experimental NeuroTherapeutics*, 14(3), 734–740. <https://doi.org/10.1007/s13311-017-0542-y>
- Johnson, M. W., Hendricks, P. S., Barrett, F. S., & Griffiths, R. R. (2019). Classic psychedelics: An integrative review of epidemiology, therapeutics, mystical experience, and brain network function. *Pharmacology & Therapeutics*, 197, 83–102. <https://doi.org/10.1016/j.pharmthera.2018.11.010>
- Johnson, S., Domínguez-García, V., Donetti, L., & Muñoz, M. A. (2014). Trophic coherence determines food-web stability. *Proceedings of the National Academy of Sciences of the United States of America*, 111(50), 17923–17928. <https://doi.org/10.1073/pnas.1409077111>
- Johnson, S., & Jones, N. S. (2017). Looplessness in networks is linked to trophic coherence. *Proceedings of the National Academy of Sciences*, 114(22), 5618–5623. <https://doi.org/10.1073/pnas.1613786114>
- Klein, A., & Tourville, J. (2012). 101 Labeled Brain Images and a Consistent Human Cortical Labeling Protocol. *Frontiers in Neuroscience*, 6. Retrieved June 14, 2023, from <https://www.frontiersin.org/articles/10.3389/fnins.2012.00171>
- Kobeleva, X., López-González, A., Kringelbach, M. L., & Deco, G. (2021). Revealing the Relevant Spatiotemporal Scale Underlying Whole-Brain Dynamics. *Frontiers in Neuroscience*, 15. Retrieved June 14, 2023, from <https://www.frontiersin.org/articles/10.3389/fnins.2021.715861>
- Kometer, M., & Vollenweider, F. X. (2016). Serotonergic Hallucinogen-Induced Visual Perceptual Alterations (A. L. Halberstadt, F. X. Vollenweider, & D. E. Nichols, Eds.). *Behavioral Neurobiology of Psychedelic Drugs*, 36, 257–282. [https://doi.org/10.1007/7854\\_2016\\_461](https://doi.org/10.1007/7854_2016_461)
- Kraehenmann, R. (2017). Dreams and Psychedelics: Neurophenomenological Comparison and Therapeutic Implications. *Current Neuropharmacology*, 15(7), 1032–1042. <https://doi.org/10.2174/1573413713666170619092629>
- Kraehenmann, R., Pokorny, D., Aicher, H., Preller, K. H., Pokorny, T., Bosch, O. G., Seifritz, E., & Vollenweider, F. X. (2017). LSD Increases Primary Process Thinking via Serotonin 2A Receptor Activation. *Frontiers in Pharmacology*, 8, 814. <https://doi.org/10.3389/fphar.2017.00814>

- Kringelbach, M. L., Cruzat, J., Cabral, J., Knudsen, G. M., Carhart-Harris, R., Whybrow, P. C., Logothetis, N. K., & Deco, G. (2020). Dynamic coupling of whole-brain neuronal and neurotransmitter systems. *Proceedings of the National Academy of Sciences of the United States of America*, 117(17), 9566–9576. <https://doi.org/10.1073/pnas.1921475117>
- Kringelbach, M. L., Perl, Y. S., Tagliazucchi, E., & Deco, G. (2023). Toward naturalistic neuroscience: Mechanisms underlying the flattening of brain hierarchy in movie-watching compared to rest and task. *Science Advances*, 9(2), eade6049. <https://doi.org/10.1126/sciadv.ade6049>
- Lebedev, A. V., Lövdén, M., Rosenthal, G., Feilding, A., Nutt, D. J., & Carhart-Harris, R. L. (2015). Finding the self by losing the self: Neural correlates of ego-dissolution under psilocybin. *Human Brain Mapping*, 36(8), 3137–3153. <https://doi.org/10.1002/hbm.22833>
- Lebedev, A., Kaelen, M., Lövdén, M., Nilsson, J., Feilding, A., Nutt, D., & Carhart-Harris, R. (2016). LSD-induced entropic brain activity predicts subsequent personality change. *Human Brain Mapping*, 37(9), 3203–3213. <https://doi.org/10.1002/hbm.23234>
- Lempel, A., & Ziv, J. (1976). On the Complexity of Finite Sequences. *IEEE Transactions on Information Theory*, 22(1), 75–81. <https://doi.org/10.1109/TIT.1976.1055501>
- Lord, L.-D., Expert, P., Atasoy, S., Roseman, L., Rapuano, K., Lambiotte, R., Nutt, D. J., Deco, G., Carhart-Harris, R. L., Kringelbach, M. L., & Cabral, J. (2019). Dynamical exploration of the repertoire of brain networks at rest is modulated by psilocybin. *NeuroImage*, 199, 127–142. <https://doi.org/10.1016/j.neuroimage.2019.05.060>
- Luppi, A. I., Carhart-Harris, R. L., Roseman, L., Pappas, I., Menon, D. K., & Stamatakis, E. A. (2021). LSD alters dynamic integration and segregation in the human brain. *NeuroImage*, 227, 117653. <https://doi.org/10.1016/j.neuroimage.2020.117653>
- Luppi, A. I., Vohryzek, J., Kringelbach, M. L., Mediano, P. A. M., Craig, M. M., Adapa, R., Carhart-Harris, R. L., Roseman, L., Pappas, I., Peattie, A. R. D., Manktelow, A. E., Sahakian, B. J., Finoia, P., Williams, G. B., Allanson, J., Pickard, J. D., Menon, D. K., Atasoy, S., & Stamatakis, E. A. (2023). Distributed harmonic patterns of structure-function dependence orchestrate human consciousness. *Communications Biology*, 6(1), 117. <https://doi.org/10.1038/s42003-023-04474-1>
- Lynn, C. W., Cornblath, E. J., Papadopoulos, L., Bertolero, M. A., & Bassett, D. S. (2021). Broken detailed balance and entropy production in the human brain. *Proceedings of the National Academy of Sciences of the United States of America*, 118(47), e2109889118. <https://doi.org/10.1073/pnas.2109889118>
- MacKay, R. S., Johnson, S., & Sansom, B. (2020). How directed is a directed network? *Royal Society Open Science*, 7(9), 201138. <https://doi.org/10.1098/rsos.201138>
- MacLean, K. A., Johnson, M. W., & Griffiths, R. R. (2011). Mystical Experiences Occasioned by the Hallucinogen Psilocybin Lead to Increases in the Personality Domain of Openness.

*Journal of psychopharmacology (Oxford, England)*, 25(11), 1453–1461. <https://doi.org/10.1177/026988111420188>

- Mallaroni, P., Mason, N. L., Kloft, L., Reckweg, J. T., Oorsouw, K. van, Toennes, S. W., Tolle, H. M., Amico, E., & Ramaekers, J. G. (2022, October 12). *Ritualistic use of ayahuasca enhances a shared functional connectome identity with others*. <https://doi.org/10.1101/2022.10.07.511268>
- Mallaroni, P., Mason, N. L., Kloft, L., Reckweg, J. T., van Oorsouw, K., & Ramaekers, J. G. (2023). Cortical structural differences following repeated ayahuasca use hold molecular signatures. *Frontiers in Neuroscience*, 17, 1217079. <https://doi.org/10.3389/fnins.2023.1217079>
- Martínez, I. A., Bisker, G., Horowitz, J. M., & Parrondo, J. M. R. (2019). Inferring broken detailed balance in the absence of observable currents. *Nature Communications*, 10(1), 3542. <https://doi.org/10.1038/s41467-019-11051-w>
- McCrae, R. R., & Costa Jr., P. T. (1997). Personality trait structure as a human universal. *American Psychologist*, 52(5), 509–516. <https://doi.org/10.1037/0003-066X.52.5.509>
- McCulloch, D. E.-W., Knudsen, G. M., Barrett, F. S., Doss, M. K., Carhart-Harris, R. L., Rosas, F. E., Deco, G., Kringelbach, M. L., Preller, K. H., Ramaekers, J. G., Mason, N. L., Müller, F., & Fisher, P. M. (2022). Psychedelic resting-state neuroimaging: A review and perspective on balancing replication and novel analyses. *Neuroscience & Biobehavioral Reviews*, 138, 104689. <https://doi.org/10.1016/j.neubiorev.2022.104689>
- McCulloch, D. E.-W., Olsen, A. S., Ozenne, B., Stenbæk, D. S., Armand, S., Madsen, M. K., Knudsen, G. M., & Fisher, P. M. (2023, July 3). *Navigating the chaos of psychedelic neuroimaging: A multi-metric evaluation of acute psilocybin effects on brain entropy*. <https://doi.org/10.1101/2023.07.03.23292164>
- Mediano, P. A. M., Ikkala, A., Kievit, R. A., Jagannathan, S. R., Varley, T. F., Stamatakis, E. A., Bekinschtein, T. A., & Bor, D. (2021, September 23). *Fluctuations in Neural Complexity During Wakefulness Relate To Conscious Level and Cognition*. <https://doi.org/10.1101/2021.09.23.461002>
- Moliner, R., Girych, M., Brunello, C. A., Kovaleva, V., Biojone, C., Enkavi, G., Antenucci, L., Kot, E. F., Goncharuk, S. A., Kaurinkoski, K., Kuutti, M., Fred, S. M., Elsilä, L. V., Sakson, S., Cannarozzo, C., Diniz, C. R. A. F., Seiffert, N., Rubiolo, A., Haapaniemi, H., ... Castrén, E. (2023). Psychedelics promote plasticity by directly binding to BDNF receptor TrkB. *Nature Neuroscience*, 26(6), 1032–1041. <https://doi.org/10.1038/s41593-023-01316-5>
- Moreno, F. A., Wiegand, C. B., Taitano, E. K., & Delgado, P. L. (2006). Safety, tolerability, and efficacy of psilocybin in 9 patients with obsessive-compulsive disorder. *The Journal of Clinical Psychiatry*, 67(11), 1735–1740. <https://doi.org/10.4088/jcp.v67n1110>
- Mueller, S., Wang, D., Fox, M. D., Thomas Yeo, B. T., Sepulcre, J., Sabuncu, M. R., Shafee, R., Lu, J., & Liu, H. (2013). Individual Variability in Functional Connectivity Architecture

- of the Human Brain. *Neuron*, 77(3), 586–595. <https://doi.org/10.1016/j.neuron.2012.12.028>
- Müller, F., Dolder, P. C., Schmidt, A., Liechti, M. E., & Borgwardt, S. (2018). Altered network hub connectivity after acute LSD administration. *NeuroImage: Clinical*, 18, 694–701. <https://doi.org/10.1016/j.nicl.2018.03.005>
- Nichols, D. E. (2016). Psychedelics (E. L. Barker, Ed.). *Pharmacological Reviews*, 68(2), 264–355. <https://doi.org/10.1124/pr.115.011478>
- Nieto-Castanon, A. (2020, February 24). *Handbook of functional connectivity Magnetic Resonance Imaging methods in CONN*. <https://doi.org/10.56441/hilbertpress.2207.6598>
- Nieto-Castanon, A. (2022, October 24). *Preparing fMRI Data for Statistical Analysis*. arXiv: 2210.13564 [q-bio]. <https://doi.org/10.48550/arXiv.2210.13564>
- Nieto-Castanon, A., & Whitfield-Gabrieli, S. (2022). *CONN functional connectivity toolbox: RRID SCR\_009550, release 22* (Version RRID SCR\_009550, release 22). Retrieved May 21, 2023, from <https://www.hilbertpress.org/link-nieto-castanon2022>
- Pagani, A., Mosquera, G., Alturki, A., Johnson, S., Jarvis, S., Wilson, A., Guo, W., & Varga, L. (2019). Resilience or robustness: Identifying topological vulnerabilities in rail networks. *Royal Society Open Science*, 6(2), 181301. <https://doi.org/10.1098/rsos.181301>
- Papo, D. (2016). Commentary: The entropic brain: A theory of conscious states informed by neuroimaging research with psychedelic drugs. *Frontiers in Human Neuroscience*, 10. Retrieved August 26, 2023, from <https://www.frontiersin.org/articles/10.3389/fnhum.2016.00423>
- Penny, W., Friston, K. J., Ashburner, J., Kiebel, S., & Nichols, T. E. (2007). Statistical Parametric Mapping: The Analysis of Functional Brain Images. Retrieved May 21, 2023, from <https://www.semanticscholar.org/paper/Statistical-Parametric-Mapping%3A-The-Analysis-of-Penny-Friston/559f06ecfe15b6f994ab6f685e9293cd43947550>
- Petermann, T., Thiagarajan, T. C., Lebedev, M. A., Nicolelis, M. A. L., Chialvo, D. R., & Plenz, D. (2009). Spontaneous cortical activity in awake monkeys composed of neuronal avalanches. *Proceedings of the National Academy of Sciences*, 106(37), 15921–15926. <https://doi.org/10.1073/pnas.0904089106>
- Petri, G., Expert, P., Turkheimer, F., Carhart-Harris, R., Nutt, D., Hellyer, P. J., & Vaccarino, F. (2014). Homological scaffolds of brain functional networks. *Journal of The Royal Society Interface*, 11(101), 20140873. <https://doi.org/10.1098/rsif.2014.0873>
- Pilgrim, C., Guo, W., & Johnson, S. (2020). Organisational Social Influence on Directed Hierarchical Graphs, from Tyranny to Anarchy. *Scientific Reports*, 10, 4388. <https://doi.org/10.1038/s41598-020-61196-8>
- Power, J. D., Mitra, A., Laumann, T. O., Snyder, A. Z., Schlaggar, B. L., & Petersen, S. E. (2014). Methods to detect, characterize, and remove motion artifact in resting state fMRI. *NeuroImage*, 84, 320–341. <https://doi.org/10.1016/j.neuroimage.2013.08.048>

- R Core Team. (2023). *R: A language and environment for statistical computing*. R Foundation for Statistical Computing. Vienna, Austria. <https://www.R-project.org/>
- Raison, C. L., Sanacora, G., Woolley, J., Heinzerling, K., Dunlop, B. W., Brown, R. T., Kakar, R., Hassman, M., Trivedi, R. P., Robison, R., Gukasyan, N., Nayak, S. M., Hu, X., O'Donnell, K. C., Kelmendi, B., Sloshower, J., Penn, A. D., Bradley, E., Kelly, D. F., ... Griffiths, R. R. (2023). Single-Dose Psilocybin Treatment for Major Depressive Disorder: A Randomized Clinical Trial. *JAMA*, 330(9), 843–853. <https://doi.org/10.1001/jama.2023.14530>
- Ramaekers, J. G., Mason, N. L., & Theunissen, E. L. (2020). Blunted highs: Pharmacodynamic and behavioral models of cannabis tolerance. *European Neuropsychopharmacology: The Journal of the European College of Neuropsychopharmacology*, 36, 191–205. <https://doi.org/10.1016/j.euroneuro.2020.01.006>
- Ramaekers, J., Mason, N., Toennes, S., Theunissen, E., & Amico, E. (2022). Functional brain connectomes reflect acute and chronic cannabis use. *Scientific Reports*, 12. <https://doi.org/10.1038/s41598-022-06509-9>
- Reid, A. T., Headley, D. B., Mill, R. D., Sanchez-Romero, R., Uddin, L. Q., Marinazzo, D., Lurie, D. J., Valdés-Sosa, P. A., Hanson, S. J., Biswal, B. B., Calhoun, V., Poldrack, R. A., & Cole, M. W. (2019). Advancing functional connectivity research from association to causation. *Nature neuroscience*, 22(11), 1751–1760. <https://doi.org/10.1038/s41593-019-0510-4>
- Riba, J., Romero, S., Grasa, E., Mena, E., Carrió, I., & Barbanoj, M. J. (2006). Increased frontal and paralimbic activation following ayahuasca, the pan-Amazonian inebriant. *Psychopharmacology*, 186(1), 93–98. <https://doi.org/10.1007/s00213-006-0358-7>
- Roseman, L., Haijen, E., Idialu-Ikato, K., Kaelen, M., Watts, R., & Carhart-Harris, R. (2019). Emotional breakthrough and psychedelics: Validation of the Emotional Breakthrough Inventory. *Journal of Psychopharmacology (Oxford, England)*, 33(9), 1076–1087. <https://doi.org/10.1177/0269881119855974>
- Roseman, L., Leech, R., Feilding, A., Nutt, D. J., & Carhart-Harris, R. L. (2014). The effects of psilocybin and MDMA on between-network resting state functional connectivity in healthy volunteers. *Frontiers in Human Neuroscience*, 8. <https://doi.org/10.3389/fnhum.2014.00204>
- Ross, S., Bossis, A., Guss, J., Agin-Liebes, G., Malone, T., Cohen, B., Mennenga, S. E., Belser, A., Kalliontzis, K., Babb, J., Su, Z., Corby, P., & Schmidt, B. L. (2016). Rapid and sustained symptom reduction following psilocybin treatment for anxiety and depression in patients with life-threatening cancer: A randomized controlled trial. *Journal of Psychopharmacology*, 30(12), 1165–1180. <https://doi.org/10.1177/0269881116675512>
- Roy, A. V., Thai, M., Klimes-Dougan, B., Westlund Schreiner, M., Mueller, B. A., Albott, C. S., Lim, K. O., Fiecas, M., Tye, S. J., & Cullen, K. R. (2021). Brain entropy and neurotrophic molecular markers accompanying clinical improvement after ketamine: Preliminary ev-

- idence in adolescents with treatment-resistant depression. *Journal of Psychopharmacology*, 35(2), 168–177. <https://doi.org/10.1177/0269881120928203>
- Ruffini, G., Damiani, G., Lozano-Soldevilla, D., Deco, N., Rosas, F. E., Kiani, N. A., Ponce-Alvarez, A., Kringelbach, M. L., Carhart-Harris, R., & Deco, G. (2023). LSD-induced increase of Ising temperature and algorithmic complexity of brain dynamics. *PLOS Computational Biology*, 19(2), e1010811. <https://doi.org/10.1371/journal.pcbi.1010811>
- Sanz Perl, Y., Bocaccio, H., Pallavicini, C., Pérez-Ipiña, I., Laureys, S., Laufs, H., Kringelbach, M., Deco, G., & Tagliazucchi, E. (2021). Nonequilibrium brain dynamics as a signature of consciousness. *Physical Review E*, 104(1-1), 014411. <https://doi.org/10.1103/PhysRevE.104.014411>
- Sarasso, S., Boly, M., Napolitani, M., Gosseries, O., Charland-Verville, V., Casarotto, S., Rosanova, M., Casali, A. G., Brichant, J.-F., Boveroux, P., Rex, S., Tononi, G., Laureys, S., & Massimini, M. (2015). Consciousness and Complexity during Unresponsiveness Induced by Propofol, Xenon, and Ketamine. *Current Biology*, 25(23), 3099–3105. <https://doi.org/10.1016/j.cub.2015.10.014>
- Seif, A., Hafezi, M., & Jarzynski, C. (2021). Machine learning the thermodynamic arrow of time. *Nature Physics*, 17(1), 105–113. <https://doi.org/10.1038/s41567-020-1018-2>
- Setsompop, K., Kimmlingen, R., Eberlein, E., Witzel, T., Cohen-Adad, J., McNab, J. A., Keil, B., Tisdall, M. D., Hoecht, P., Dietz, P., Cauley, S. F., Tountcheva, V., Matschl, V., Lenz, V. H., Heberlein, K., Potthast, A., Thein, H., Van Horn, J., Toga, A., ... Wald, L. L. (2013). Pushing the limits of in vivo diffusion MRI for the Human Connectome Project. *NeuroImage*, 80, 220–233. <https://doi.org/10.1016/j.neuroimage.2013.05.078>
- Shew, W. L., & Plenz, D. (2013). The functional benefits of criticality in the cortex. *The Neuroscientist: A Review Journal Bringing Neurobiology, Neurology and Psychiatry*, 19(1), 88–100. <https://doi.org/10.1177/1073858412445487>
- Shew, W. L., Yang, H., Petermann, T., Roy, R., & Plenz, D. (2009). Neuronal Avalanches Imply Maximum Dynamic Range in Cortical Networks at Criticality. *Journal of Neuroscience*, 29(49), 15595–15600. <https://doi.org/10.1523/JNEUROSCI.3864-09.2009>
- Shinozuka, K., Jerotic, K., Mediano, P., Zhao, A. T., Preller, K. H., Carhart-Harris, R., & Kringelbach, M. L. (2023, October 7). *The Hierarchy of Psychedelic Effects: Three Systematic Reviews and Meta-Analyses*. <https://doi.org/10.1101/2023.10.06.561183>
- Singleton, S. P., Luppi, A. I., Carhart-Harris, R. L., Cruzat, J., Roseman, L., Nutt, D. J., Deco, G., Kringelbach, M. L., Stamatakis, E. A., & Kuceyeski, A. (2022). Receptor-informed network control theory links LSD and psilocybin to a flattening of the brain's control energy landscape. *Nature Communications*, 13(1), 5812. <https://doi.org/10.1038/s41467-022-33578-1>
- Sladky, R., Friston, K. J., Tröstl, J., Cunnington, R., Moser, E., & Windischberger, C. (2011). Slice-timing effects and their correction in functional MRI. *NeuroImage*, 58(2), 588–594. <https://doi.org/10.1016/j.neuroimage.2011.06.078>

- Sporns, O., & Betzel, R. F. (2016). Modular Brain Networks. *Annual Review of Psychology*, 67(1), 613–640. <https://doi.org/10.1146/annurev-psych-122414-033634>
- Tagliazucchi, E., Carhart-Harris, R., Leech, R., Nutt, D., & Chialvo, D. R. (2014). Enhanced repertoire of brain dynamical states during the psychedelic experience. *Human Brain Mapping*, 35(11), 5442–5456. <https://doi.org/10.1002/hbm.22562>
- Tagliazucchi, E., Roseman, L., Kaelen, M., Orban, C., Muthukumaraswamy, S. D., Murphy, K., Laufs, H., Leech, R., McGonigle, J., Crossley, N., Bullmore, E., Williams, T., Bolstridge, M., Feilding, A., Nutt, D. J., & Carhart-Harris, R. (2016). Increased Global Functional Connectivity Correlates with LSD-Induced Ego Dissolution. *Current biology: CB*, 26(8), 1043–1050. <https://doi.org/10.1016/j.cub.2016.02.010>
- Tewarie, P. K. B., Hindriks, R., Lai, Y. M., Sotiropoulos, S. N., Kringselbach, M., & Deco, G. (2023). Non-reversibility outperforms functional connectivity in characterisation of brain states in MEG data. *NeuroImage*, 276. <https://doi.org/10.1016/j.neuroimage.2023.120186>
- Timmermann, C., Roseman, L., Haridas, S., Rosas, F. E., Luan, L., Kettner, H., Martell, J., Erritzoe, D., Tagliazucchi, E., Pallavicini, C., Girn, M., Alamia, A., Leech, R., Nutt, D. J., & Carhart-Harris, R. L. (2023). Human brain effects of DMT assessed via EEG-fMRI. *Proceedings of the National Academy of Sciences*, 120(13), e2218949120. <https://doi.org/10.1073/pnas.2218949120>
- Timmermann, C., Roseman, L., Schartner, M., Milliere, R., Williams, L. T. J., Erritzoe, D., Muthukumaraswamy, S., Ashton, M., Bendrioua, A., Kaur, O., Turton, S., Nour, M. M., Day, C. M., Leech, R., Nutt, D. J., & Carhart-Harris, R. L. (2019). Neural correlates of the DMT experience assessed with multivariate EEG. *Scientific Reports*, 9(1), 16324. <https://doi.org/10.1038/s41598-019-51974-4>
- Varley, T. F., Carhart-Harris, R., Roseman, L., Menon, D. K., & Stamatakis, E. A. (2020). Serotonergic psychedelics LSD & psilocybin increase the fractal dimension of cortical brain activity in spatial and temporal domains. *NeuroImage*, 220, 117049. <https://doi.org/10.1016/j.neuroimage.2020.117049>
- Viol, A., Palhano-Fontes, F., Onias, H., De Araujo, D. B., & Viswanathan, G. M. (2017). Shannon entropy of brain functional complex networks under the influence of the psychedelic Ayahuasca. *Scientific Reports*, 7(1), 7388. <https://doi.org/10.1038/s41598-017-06854-0>
- Wang, Q., Wu, Q., Wang, J., Chen, Y., Zhang, G., Chen, J., Zhao, J., & Wu, P. (2017). Ketamine Analog Methoxetamine Induced Inflammation and Dysfunction of Bladder in Rats. *International Journal of Molecular Sciences*, 18(1), 117. <https://doi.org/10.3390/ijms18010117>
- Weber. (2010). Htr2a gene and 5-HT2A receptor expression in the cerebral cortex studied using genetically modified mice. *Frontiers in Neuroscience*. <https://doi.org/10.3389/fnins.2010.00036>

- Whitfield-Gabrieli, S., & Nieto-Castanon, A. (2012). Conn: A functional connectivity toolbox for correlated and anticorrelated brain networks. *Brain Connectivity*, 2(3), 125–141. <https://doi.org/10.1089/brain.2012.0073>
- Whitfield-Gabrieli, S., Nieto-Castanon, A., & Ghosh, S. (2011). *Artifact detection tools (ART)* (Version Release Version 7(19), 11). Cambridge, MA.
- Wickham, H., Averick, M., Bryan, J., Chang, W., McGowan, L. D., François, R., Grolemund, G., Hayes, A., Henry, L., Hester, J., Kuhn, M., Pedersen, T. L., Miller, E., Bache, S. M., Müller, K., Ooms, J., Robinson, D., Seidel, D. P., Spinu, V., ... Yutani, H. (2019). Welcome to the tidyverse. *Journal of Open Source Software*, 4(43), 1686. <https://doi.org/10.21105/joss.01686>
- Yeo, B. T., Krienen, F. M., Sepulcre, J., Sabuncu, M. R., Sabuncu, M. R., Lashkari, D., Hollinshead, M. O., Roffman, J. L., Smoller, J. W., Zöllei, L., Polimeni, J. R., Fischl, B., Liu, H., & Buckner, R. L. (2011). The organization of the human cerebral cortex estimated by intrinsic functional connectivity. *Journal of Neurophysiology*, 106(3), 1125–1165. <https://doi.org/10.1152/jn.00338.2011>  
MAG ID: 2067456724.
- Zhang, X. S., Roy, R. J., & Jensen, E. W. (2001). EEG complexity as a measure of depth of anesthesia for patients. *IEEE transactions on bio-medical engineering*, 48(12), 1424–1433. <https://doi.org/10.1109/10.966601>
- Ziv, J., & Lempel, A. (1977). A universal algorithm for sequential data compression. *IEEE Transactions on Information Theory*, 23(3), 337–343. <https://doi.org/10.1109/TIT.1977.1055714>

## **Supplemental Figures**

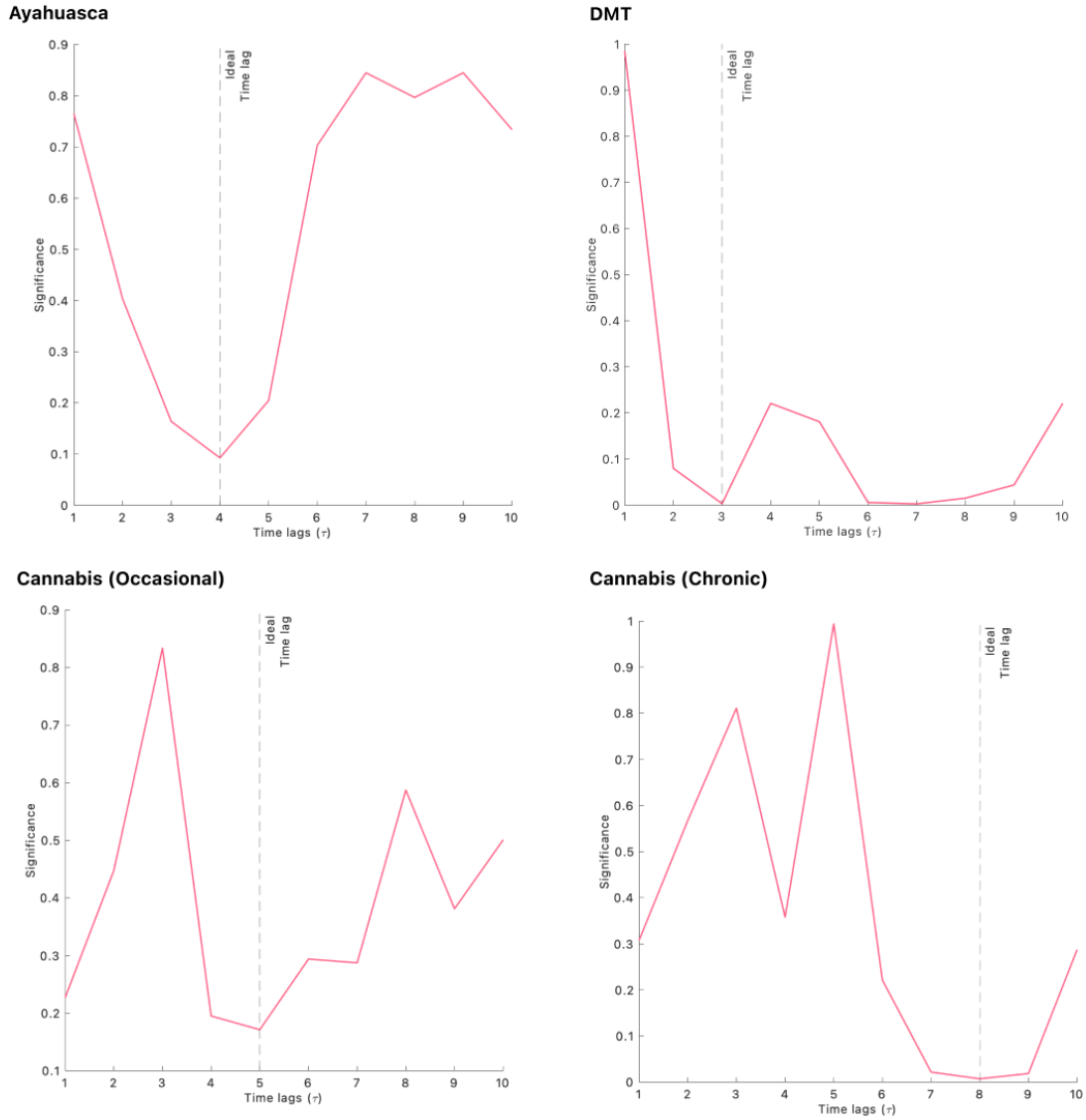


Figure A.1: Evaluation of the ideal time-delay constant  $\tau$  for each condition. Model-free irreversibility was calculated for Tau values 1 through 10 for each condition. For ayahuasca, occasional and chronic use of cannabis, a Wilcoxon rank-sum test was used to evaluate significance. The ideal Tau was determined as the most sensitive measure which best discriminates between baseline or placebo and drug conditions. For DMT, a mixed effects model was used in order to account for the pre-injection data as a covariate.

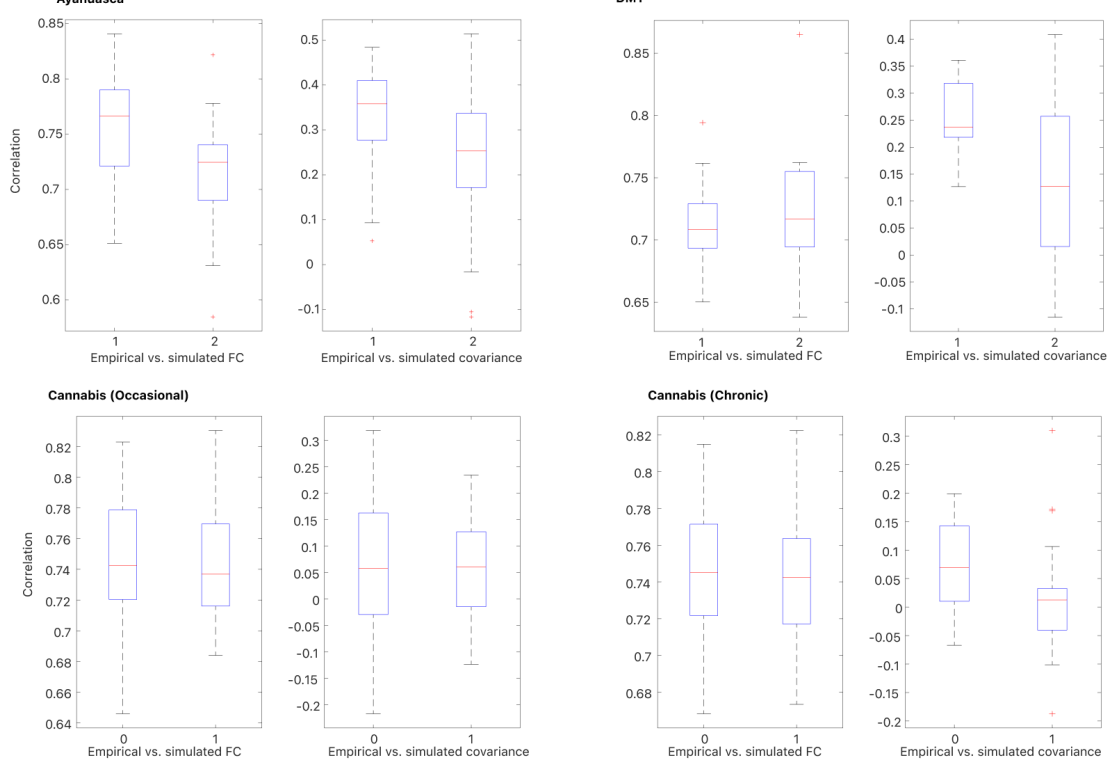


Figure A.2: Correlations between empirical and simulated functional connectivity (left panel, each condition), and between empirical and simulated covariance of irreversibility matrices (right panel, each condition). "1" indicates baseline or placebo condition. "2" indicates drug condition.

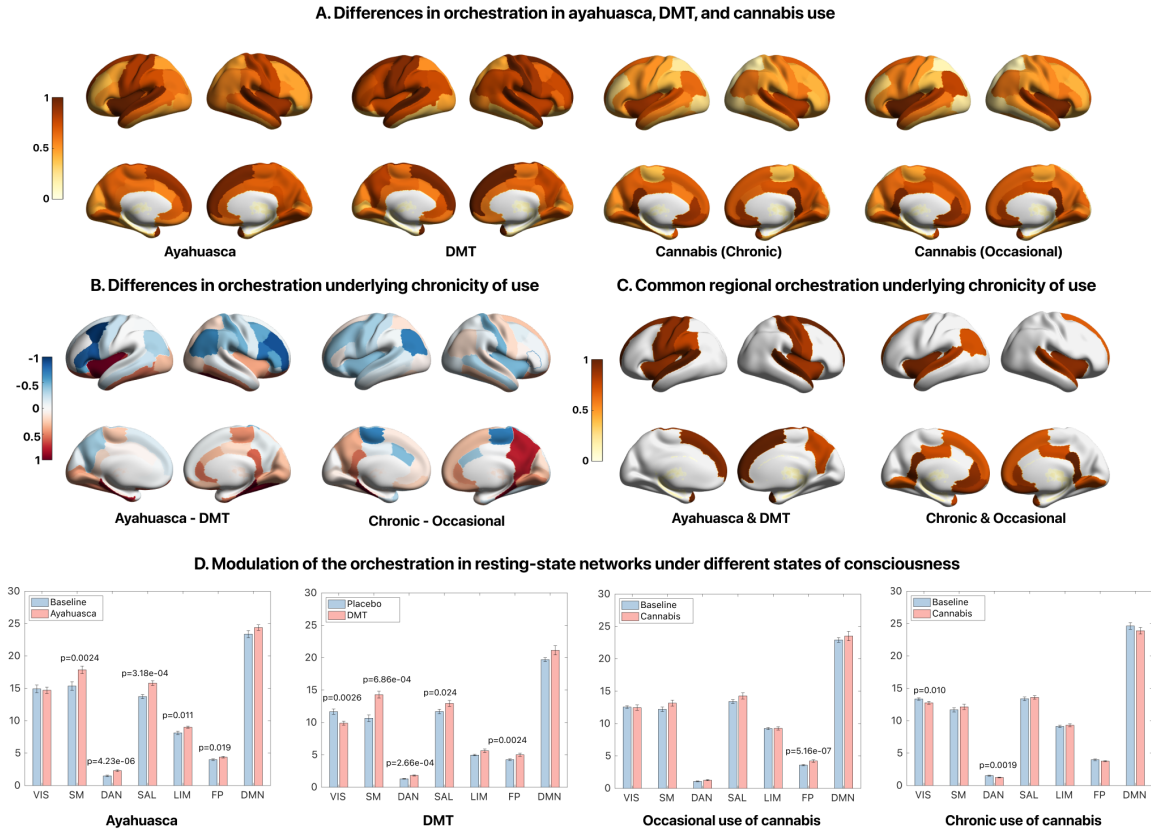


Figure A.3: Differences in orchestration, a measure of total directed connectivity, under psychedelics and cannabis. (A) Measure of orchestration for each drug condition. Significant orchestrators for ayahuasca and DMT include bilateral pre- and post-central, insula, and superior frontal. For cannabis, bilateral insula, isthmus cingulate, and caudal anterior cingulate were found to be more connected than other regions in the brain. (B) Differences in orchestration between psychedelics, ayahuasca and DMT, and chronic and occasional use of cannabis. (C) Common orchestrators under psychedelics and cannabis. (D) Modulation of network-level orchestration under psychedelics and cannabis. Non-parametric permutation testing (5,000 iterations, threshold = 0.01) was utilized to evaluate changes in individual resting-state networks for each drug condition.

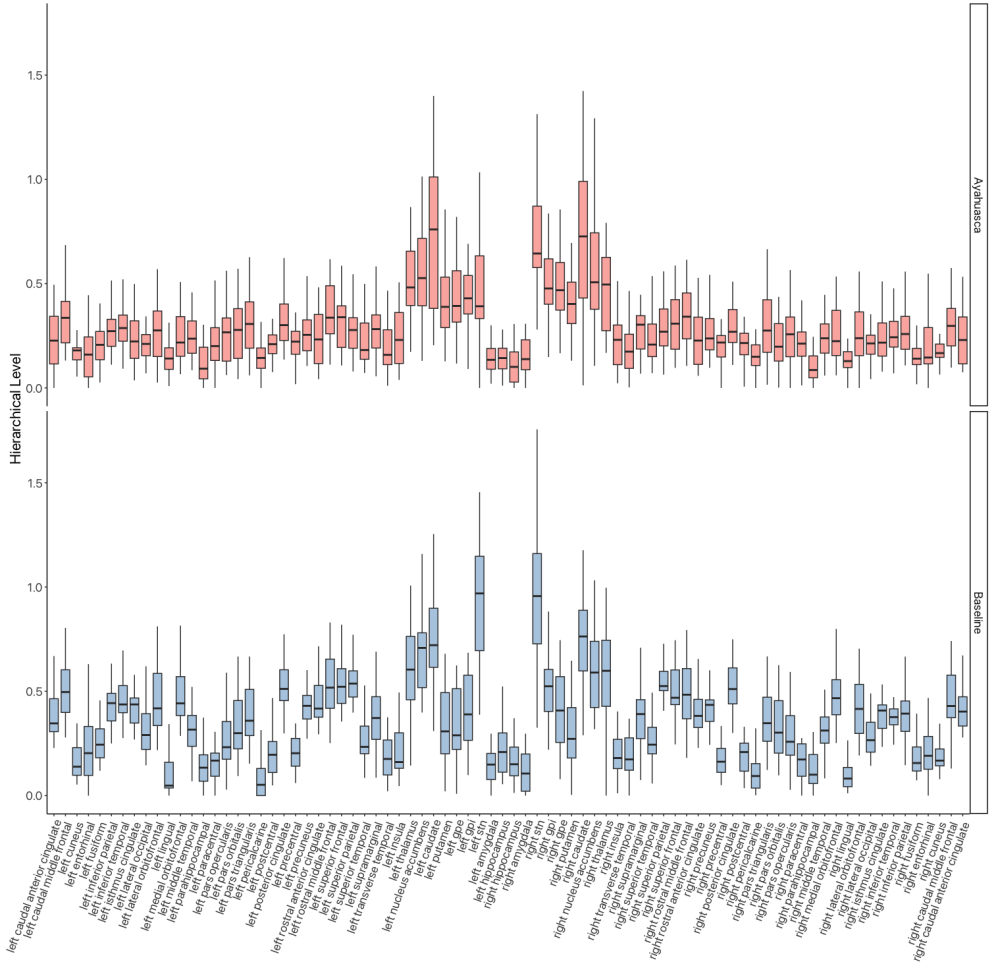


Figure A.4: Hierarchical levels for each region in the DBS80 across baseline and ayahuasca conditions. Top panel, ayahuasca. Bottom panel, baseline.

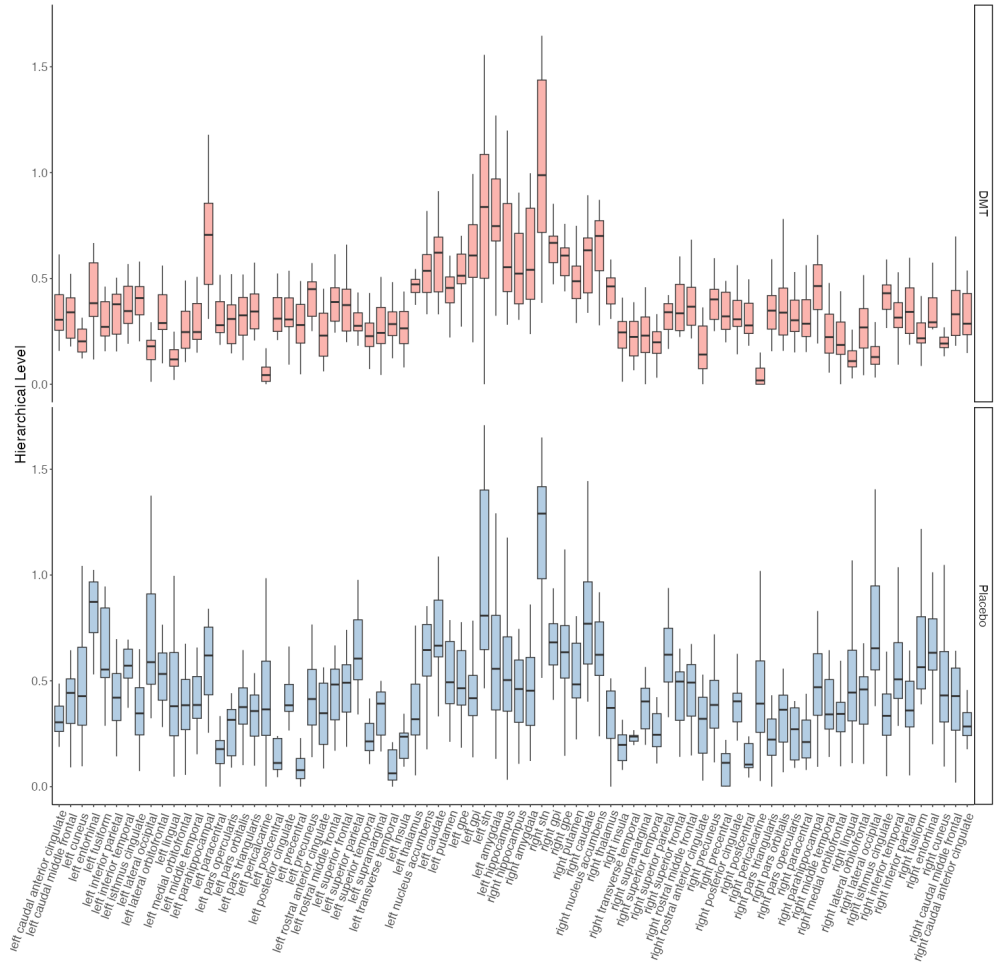


Figure A.5: Hierarchical levels for each region in the DBS80 across placebo and DMT conditions. Top panel, DMT. Bottom panel, placebo.

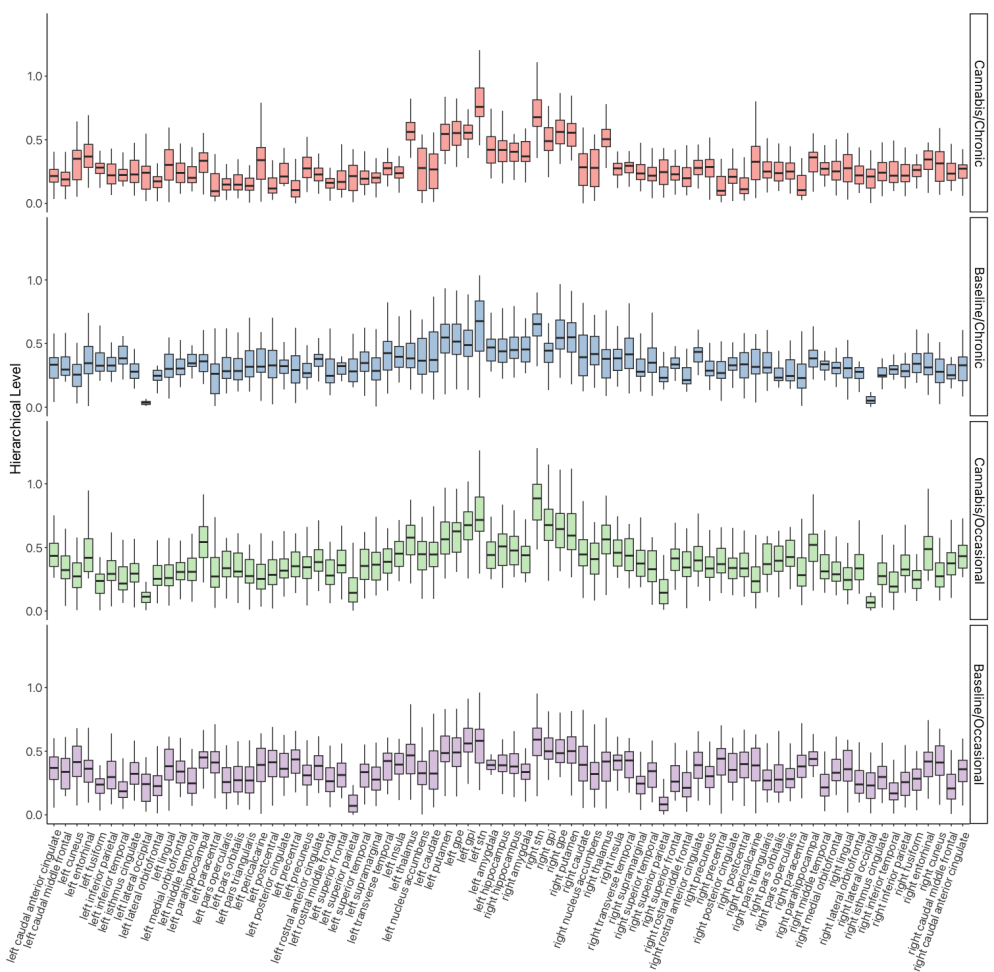


Figure A.6: Hierarchical levels for each region in the DBS80 across baseline and cannabis (both chronic and occasional users). Top panel, cannabis in chronic users. Mid-top panel, baseline in chronic users. Mid-bottom panel, cannabis in occasional users. Bottom panel, baseline in occasional users.